

Complexes of copper(II) with 3-(*ortho*-substituted phenylhydrazo)pentane-2,4-diones: syntheses, properties and catalytic activity for cyclohexane oxidation†

Maximilian N. Kopylovich,^a Andreia C. C. Nunes,^a Kamran T. Mahmudov,^a Matti Haukka,^b Tatiana C. O. Mac Leod,^a Luísa M. D. R. S. Martins,^{a,c} Maxim L. Kuznetsov^a and Armando J. L. Pombeiro^{a*}

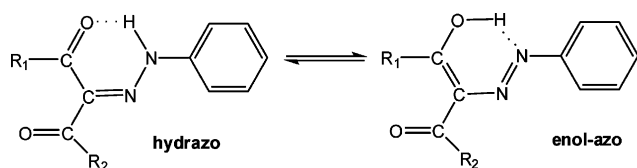
Received 3rd November 2010, Accepted 21st December 2010

DOI: 10.1039/c0dt01527j

Reactions of copper(II) with 3-phenylhydrazopentane-2,4-diones X-2-C₆H₄-NHN=C{C(=O)CH₃}₂ bearing a substituent in the *ortho*-position [X = OH (H₃L¹) **1**, AsO₃H₂ (H₃L²) **2**, Cl (HL³) **3**, SO₃H (H₂L⁴) **4**, COOCH₃ (HL⁵) **5**, COOH (H₂L⁶) **6**, NO₂ (HL⁷) **7** or H (HL⁸) **8**] lead to a variety of complexes including the monomeric [CuL⁴(H₂O)₂]-H₂O **10**, [CuL⁴(H₂O)₂] **11** and [Cu(HL⁴)₂(H₂O)₄] **12**, the dimeric [Cu₂(H₂O)₂(μ-HL²)₂] **9** and the polymeric [Cu(μ-L⁶)_n] **13** ones, often bearing two fused six-membered metallacycles. Complexes **10**–**12** can interconvert, depending on pH and temperature, whereas the Cu(II) reactions with **4** in the presence of cyanoguanidine or imidazole (**im**) afford the monomeric compound [Cu(H₂O)₄{NCNC(NH₂)₂}₂](HL⁴)₂·6H₂O **14** and the heteroligand polymer [Cu(μ-L⁴)(**im**)_n] **15**, respectively. The compounds were characterized by single crystal X-ray diffraction (complexes), electrochemical and thermogravimetric studies, as well as elemental analysis, IR, ¹H and ¹³C NMR spectroscopies (diones) and ESI-MS. The effects of the substituents in **1**–**8** on the HOMO–LUMO gap and the relative stability of the model compounds [Cu(OH)(L⁸)(H₂O)]·H₂O, [Cu(L¹)(H₂O)₂]·H₂O and [Cu(L⁴)(H₂O)₂]·H₂O are discussed on the basis of DFT calculations that show the stabilization follows the order: two fused 6-membered > two fused 6-membered/5-membered > one 6-membered metallacycles. Complexes **9**, **10**, **12** and **13** act as catalyst precursors for the peroxidative oxidation (with H₂O₂) of cyclohexane to cyclohexanol and cyclohexanone, in MeCN/H₂O (total yields of ca. 20% with TONs up to 566), under mild conditions.

Introduction

3-Phenylhydrazopentane-2,4-diones are azoderivatives of β-diketones (ADB) (Scheme 1)¹ potentially with a wide range of applications,² e.g. they can be used as optical recording media and



Scheme 1

^aCentro de Química Estrutural, Complexo I, Instituto Superior Técnico, TU Lisbon, Av. Rovisco Pais, 1049-001, Lisbon, Portugal. E-mail: pombeiro@ist.utl.pt

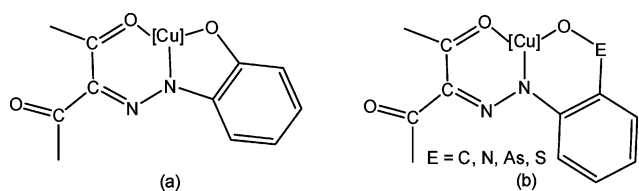
^bUniversity of Joensuu, Department of Chemistry, P.O. Box 111, FIN-80101, Joensuu, Finland

^cÁrea Departamental de Engenharia Química, ISEL, R. Conselheiro Emídio Navarro, 1959-007, Lisboa, Portugal

† Electronic supplementary information (ESI) available. CCDC reference numbers 798948–798954. For ESI and crystallographic data in CIF or other electronic format see DOI: 10.1039/c0dt01527j

spin-coating films³ or be applied for further organic synthesis.⁴ *ortho*-Hydroxy substituted ADB were effectively applied for the selective determination of copper(II) and iron(III) in various industrial and natural objects.⁵ It was assumed that these compounds can exist in several tautomeric forms, and that the tautomeric equilibria can play an important role for applications e.g. as bistate molecular switches⁶ or regulation of the selectivity of analytical reactions.^{5b} The hydrazo ⇌ enol-azo tautomeric transitions are connected with a π-electron delocalization within a so-called “resonance assisted hydrogen bond” (RAHB).^{6a,7} Usually, in the solid phase all the structurally studied ADB are stabilized in the hydrazo form,^{6,8} while in solution the investigated unsymmetrical ADB can exist as a mixture of enol-azo and hydrazo tautomers.^{8c}

In spite of the above interest in ADB compounds, their coordination chemistry still remains underdeveloped, although some complexes e.g. with copper(II), nickel(II) or sodium(I) have been reported^{8b,c} and we have synthesized^{8d,e} a few copper(II) compounds with *ortho*-hydroxy substituted phenylhydrazo-β-diketones containing fused six- and five-membered metallacycles (Scheme 2a). We can anticipate that the five-membered metallacycle is under a higher tension than the six-membered cycle and that the complexes with a six-membered ring may be more stable.



Scheme 2

This could be achieved by the introduction of a suitable functional group, e.g. $-\text{AsO}_3\text{H}_2$, $-\text{SO}_3\text{H}$, $-\text{COOCH}_3$, $-\text{COOH}$ or $-\text{NO}_2$, into the *ortho*-position of the aromatic part of the hydrazone moiety (Scheme 2b), and such an approach was followed in the present study.

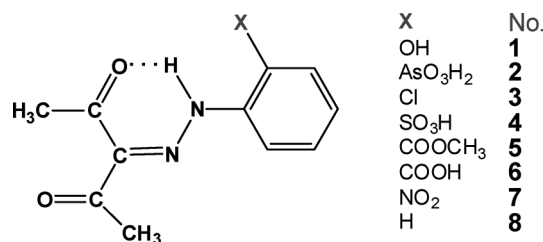
On the other hand, some copper(II)-ADB complexes have been successfully applied as catalysts for a few oxidation reactions, in particular the peroxidative oxidation of cyclohexane,^{8d,e} Functionalization of saturated hydrocarbons under mild conditions and using environmentally friendly oxidants is currently an area of great interest.⁹ Different catalysts have been developed, and, among them, copper-containing complexes¹⁰ are of a high potential interest, since copper is present in the active sites of several oxidation enzymes, including the multi-copper particulate methane monooxidase (PMMO),¹¹ is cheap and widespread in Nature. Hence, it would be particularly attractive to check the catalytic activity of the synthesized copper(II) complexes in the above type of alkane oxidation reaction.

Thus, in this work we focused on the following aims: *i*) to include $-\text{AsO}_3\text{H}_2$, $-\text{SO}_3\text{H}$, $-\text{COOCH}_3$, $-\text{COOH}$ and $-\text{NO}_2$ substituents into the *ortho*-position of the aromatic ring of ADB; *ii*) to study the influence of these substituents on the tautomeric balance and coordination ability of the corresponding ligands, namely towards copper(II), with the formation of two fused six-membered metallacycles; *iii*) to study some physicochemical properties of the ligands and complexes; *iv*) to check the potential of the synthesized complexes for further transformations; *v*) to apply the complexes as catalyst precursors for the peroxidative oxidation of cyclohexane.

Results and discussion

Synthesis and properties of 3-(*ortho*-substituted phenylhydrazo)pentane-2,4-diones

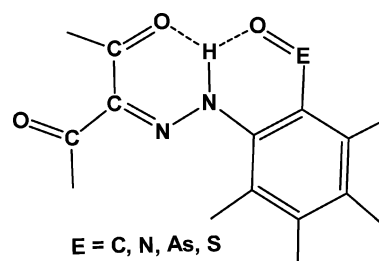
The 3-(*ortho*-substituted phenylhydrazo)pentane-2,4-diones of this study (Scheme 3) were prepared by a modified (see Experimental) known¹ aqueous diazotization of corresponding amines with subsequent coupling with pentane-2,4-dione. Compounds 2–5 are novel but, for comparative purposes, we also synthesized



Scheme 3

and studied the related 1 and 6–8, whose preparation and some properties have been reported earlier.^{8,12}

The ADB compounds can potentially exist in three (hydrazo, enol-azo and keto-azo) tautomeric forms,^{5,8} but experimental data testify that 1–8 are stabilized in the hydrazo form. In fact, their ¹H-NMR spectra in DMSO-*d*₆ solution at room temperature show only one signal at δ 12.4–15.7 which can be assigned to the proton of the protonated nitrogen atom adjacent to the aryl unit ($=\text{N}-\text{NH}-$ hydrazo form), while the two methyl groups of the pentane-2,4-dione moiety yield separate singlets on account of the formation of an hydrogen bond between one carbonyl group and the NH of the hydrazone moiety.^{6,8,12} Weak $\text{N}-\text{H}\cdots\text{O}$ bonds are known to give $\delta_{\text{N-H}}$ values in the 7–9 range, while chemical shifts of 12 ppm and higher are characteristic of a bifurcated (three-centre) H-bond (Scheme 4).¹² Thus, compounds 1–8 bear such a three-centre H-bond in solution, what is also supported, in the solid state, by X-ray diffraction analysis of 6^{12a} and by their IR data: $\nu(\text{NH})$ 3069–3482 cm^{-1} , $\nu(\text{C}=\text{O})$ 1678–1638 cm^{-1} , $\nu(\text{C}=\text{O}\cdots\text{H})$ 1646–1601 cm^{-1} and $\nu(\text{C}=\text{N})$ 1601–1575 cm^{-1} .



Scheme 4

By cyclic voltammetry at a Pt disc electrode, in 0.2 M $[\text{nBu}_4\text{N}][\text{BF}_4]/\text{NCMe}$, at room temperature, the ADB compounds 1–8 exhibit one irreversible oxidation wave (I^{ox}) and one irreversible reduction wave (I^{red}) (Fig. 1, for 8) at half-peak potential ($E_{\text{p}/2}^{\text{ox}}$ and $E_{\text{p}/2}^{\text{red}}$) values (*versus* SCE) given in Table 1. In the case of 7, the reduction wave of the nitro group is observed at $E_{\text{p}}^{\text{red}} = -0.92$ V. Exhaustive controlled potential electrolysis (CPE) at a potential slightly anodic (or cathodic, for the reduction) to that

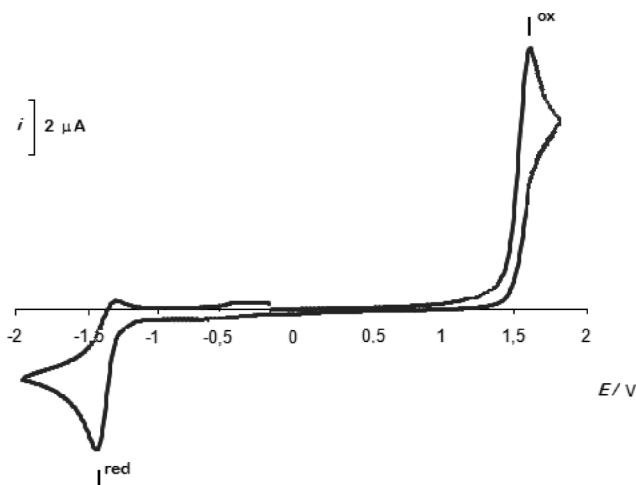


Fig. 1 Cyclic voltammogram ($\nu = 0.2 \text{ V s}^{-1}$) of a 4.1 mM solution of 8, initiated by the anodic sweep, in 0.2 M $[\text{nBu}_4\text{N}][\text{BF}_4]/\text{NCMe}$, at a platinum disc electrode ($d = 0.5 \text{ mm}$).

Table 1 Cyclic voltammetric data,^a calculated vertical ionization potentials and electron affinities for **1–8**

Compound	$E_{p/2}^{\text{ox}}$	IP ^b	$E_{p/2}^{\text{red}}$	EA ^c
1	1.23	7.76	-0.87	0.95
2	— ^d	8.13	— ^d	1.14
3	1.65	8.09	-1.23	1.19
4	1.36	8.46	-1.27	1.62
5	1.59	7.98	-1.25	1.14
6	1.61	8.09	-1.46	1.23
7^e	1.80	8.46	-1.30	1.80
8	1.49	8.00	-1.35	1.05

^a Values given in V \pm 0.02 relative to the SCE, scan rate = 0.2 V s⁻¹; ^b calculated vertical ionization potentials in eV; ^c calculated vertical electron affinities in eV; ^d no wave has been observed under the experimental conditions of this study; ^e an irreversible reduction wave is also observed at $E_p^{\text{red}} = -0.92$ V due to the reduction of the nitro group.

of the peak potential indicates the occurrence of a single-electron oxidation or of a two-electron reduction at the corresponding waves, during the extended time scale of CPE.

In general, the values of the oxidation potential of **1–8** reflect the electron-acceptor character of the substituent, the former tending to increase with the latter, but no clear relationship with the Hammett's σ_o or σ_p or any other related constant was found, conceivably due to the irreversibility of the redox processes. This contrasts with the case of the *para*-substituted ADB for which we have recently reported¹³ a correlation between the polar conjugation σ_p^- substituent constant and the oxidation potential.

Quantum-chemical calculations performed at the B3LYP level of theory demonstrate that the main contribution to the HOMO of **1–8** comes from orbitals of the C(3) and N(9) atoms and of the phenyl group (Fig. 2, Table S2[†]). The LUMO is centred on the C(2), C(3), C(4), and N(9) atoms. Additionally, orbitals of N(7) (**1–6** and **8**) or C(10) (**2**, **4–7**) atoms and of the NO₂ group (**7**) give a noticeable contribution to the LUMO. The calculated vertical ionization potential values roughly correlate with the experimental

oxidation potentials except for **4** which, according to the theory, should be much harder to oxidize than was observed (Table 1). There is no satisfactory correlation between the calculated vertical electron affinities and the experimental reduction potential values, the irreversible character of the reduction being conceivably the reason of the discrepancy.

It is known that azodyes, and in particular ADB, can be used for optical data storage³ and that the knowledge of thermal properties is important for such applications. Hence, differential thermal analyses of **1**, **2**, **4**, **6** and **8** were performed (Fig. S1 and S2, Table S3[†]). Compound **1** is thermally stable until 470 K, when an endothermic decomposition occurs with the maximum mass loss at 527 K. **2** decomposes in three successive steps: the first one in the 343–388 K range can be attributed to the loss of the hydrate water molecules, the second one occurs at 466–504 K and the third one with maximum mass loss at 575 K. **4** also decomposes in three steps: dehydration at 356 K and decomposition in the 486–561 and 643–701 K intervals. **6** starts to decompose at 491 K, indicating the absence of adsorptive water molecules. The calculated Gibbs free energy of the decomposition of **6** (the calculation details are given in ESI, Fig. S1 and S2, Table S3[†]) is mainly contributed to by the enthalpy factor with an overall process similar to that of **1**. The decomposition of **8** occurs at 414–517 K showing a strong and sharp DTG peak at 499 K with a strong mass loss (82.5%) and a high activation energy ($E_a = 69.2$ kJ mol⁻¹). Some of the ligands are quite thermally stable (**1**, **6** and **8**), and this feature, the high weight loss rate and the sharp thermal decomposition threshold make the studied compounds potential candidates for optical recording materials.³

Syntheses and characterization of copper(II) complexes

Copper(II) complexes derived from reactions with **2**, **4**, **6** were isolated and characterized by elemental analysis, ESI-MS⁺ and IR spectroscopy, single crystal X-ray diffraction and thermogravimetry. A slow evaporation of a mixture of copper(II) nitrate hydrate

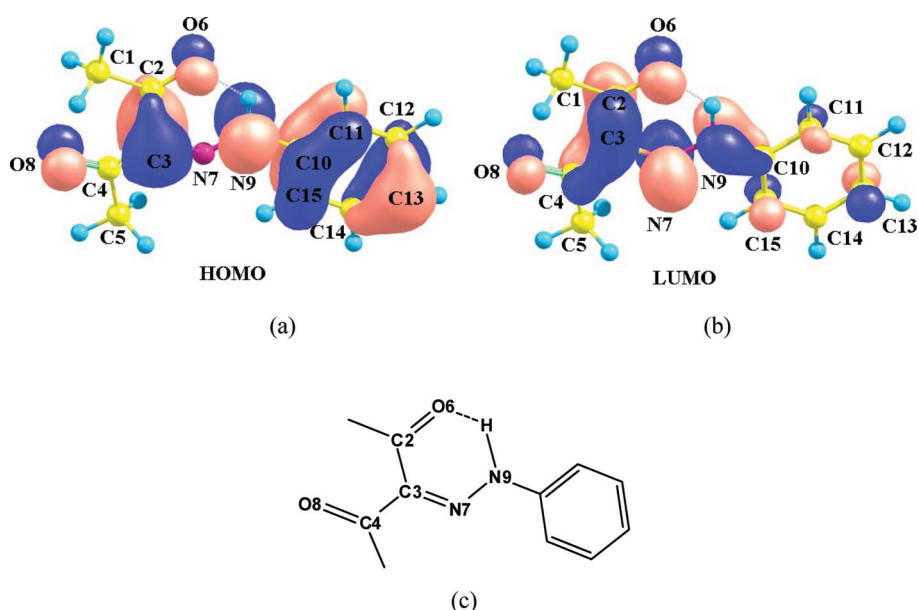
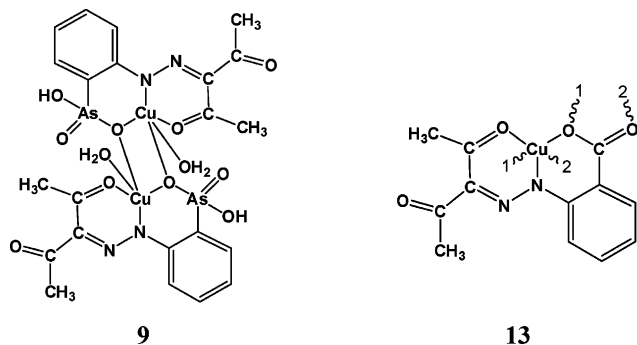


Fig. 2 Plots of the HOMO (a) and LUMO (b) of **8** with atom labelling scheme (c).

and **2** in water furnishes greenish–black crystals of the dimeric complex $[\text{Cu}_2(\mu\text{-HL}^2)_2(\text{H}_2\text{O})_2]$ (**9**) (Scheme 5). Elemental analysis and ESI-MS⁺ peak at 389.8 support the formulation, while IR reveals $\nu(\text{OH})$, $\nu(\text{C}=\text{O})$ and $\nu(\text{C}=\text{N})$ at 3368, 1660 and 1557 cm^{-1} , respectively.



Scheme 5

The dimer **9** crystallizes in the triclinic space group $P\bar{1}$ comprising of one half of the complex molecule in the asymmetric entity of the unit cell (Fig. 3a). The coordination environment $\text{Cu}(1)\text{O}(1)\text{O}(5)\text{N}(1)$ of the copper ion is of a distorted square planar geometry with the $\text{Cu}-\text{O}(1)$, $\text{Cu}-\text{O}(5)$ and $\text{Cu}-\text{N}(1)$ distances being 1.9760(19), 1.900(2) and 1.991(2) Å, respectively (Table 2). The pentacoordinated copper(II) atoms belong to three different metallacycles: one central planar endo Cu_2O_2 core and two fused six-membered exo rings. In the Cu_2O_2 core the $\text{Cu}1$ and $\text{Cu}1\#1$ centroid...centroid distance is of 3.109 Å. To diminish any intramolecular strain, the aromatic rings are arranged approximately perpendicular (83.5°) with respect to the CuO_2N plane. The complex formation causes a decrease in the $\text{C}(10)-\text{O}(5)$ bond length (1.255(3) Å), whereas the $\text{C}(10)-\text{C}(7)$ bond (1.444(4) Å) is significantly lengthened, indicating a change of the π -electron distribution within the pentane-2,4-dione fragment. $\text{C}(8)-\text{O}(4)$ (1.225(4) Å) is shorter than $\text{C}(10)-\text{O}(5)$ (1.255(3) Å) due to coordination of $\text{O}(5)$ to copper(II). In addition, the free carbonyl oxygen is associated with the coordinated water hydrogen $\text{H}(\text{O}6)$ of an adjacent molecule ($\text{H}\cdots\text{O}=\text{C}$, 2.741 Å).

In the packing structure of **9** (Fig. S4†), the observed mode of the molecular cross-linking is favoured by an inclination of neighbouring molecules which, however, prevent aromatic interactions. A different structural motif is found in the $\text{Cu}(\text{II})$ complex with a H_2L^1 derived ligand,^{8c} which crystallizes from methanol as the dimer $[\text{Cu}_2(\mu\text{-L}^1)_2(\text{CH}_3\text{OH})_2]$ with the methanol molecules located on the vertex of the quadratic-pyramidal coordination sphere of the copper(II) ion. In the latter case, the packing structure is determined by the coordination behaviour of the water molecule, leading to $\text{O}-\text{H}\cdots\text{O}$ bonded molecular zigzag strands which are further associated by the edge-to-face aromatic interactions.

The thermal behaviour of **9** relates to its structure. Under heating, it decomposes in four consecutive steps (Fig. S3b,† Table 3). The first one, in the 454–499 K range, with a strong and sharp DTG peak at 465 K, most probably concerns the vigorous elimination of the coordinated water molecules with an activation energy of 58 kJ mol^{-1} . In the second step (with 33.3% weight loss), part of the ligand is destroyed with an endothermic peak at 535 K. The third and fourth steps of the decomposition bear high positive $\Delta^\ddagger G$ values in the 590–622 and 711–716 K ranges, respectively. All the steps proceed with a negative $\Delta^\ddagger S$ suggesting a low rate of the thermal decomposition.¹⁴

A slow evaporation of a solution of copper(II) nitrate hydrate and **6** in acetone–water (4:1, v/v) furnishes greenish–black crystals of **13** (Scheme 5). Elemental analysis and IR spectrum support the formulation of $[\text{Cu}(\mu\text{-L}^6)]_n$, which is also confirmed by X-ray diffraction analyses. Hence, complex **13** is a 1D polymer formed by coordination of a carboxyl group to copper(II) (Fig. 3b) containing a crystallographically imposed centre of inversion. The coordination sphere of the penta-coordinated copper(II) is best described as distorted square-pyramidal. The copper atom is shifted towards the apical position above the basal $\text{O}(5)-\text{N}(1)-\text{O}(7)-\text{O}(6i)$ plane; this apical position is occupied by a coordinated carboxyl group of an adjacent molecule, thus one monomer is perpendicular to other. The copper(II) ion belongs to three different metallacycles: the first $\text{C}(12)-\text{O}(6)-\text{Cu}(1)-\text{O}(7)$ core, which bridges to the neighbour molecule, and $\text{Cu}(1)-\text{N}(1)-\text{N}(2)-\text{C}(7)-\text{C}(10)-\text{O}(5)$ and $\text{Cu}(1)-\text{N}(1)-\text{C}(5)-\text{C}(1)-\text{C}(12)-\text{O}(7)$ two six-membered fused metallacycles. The

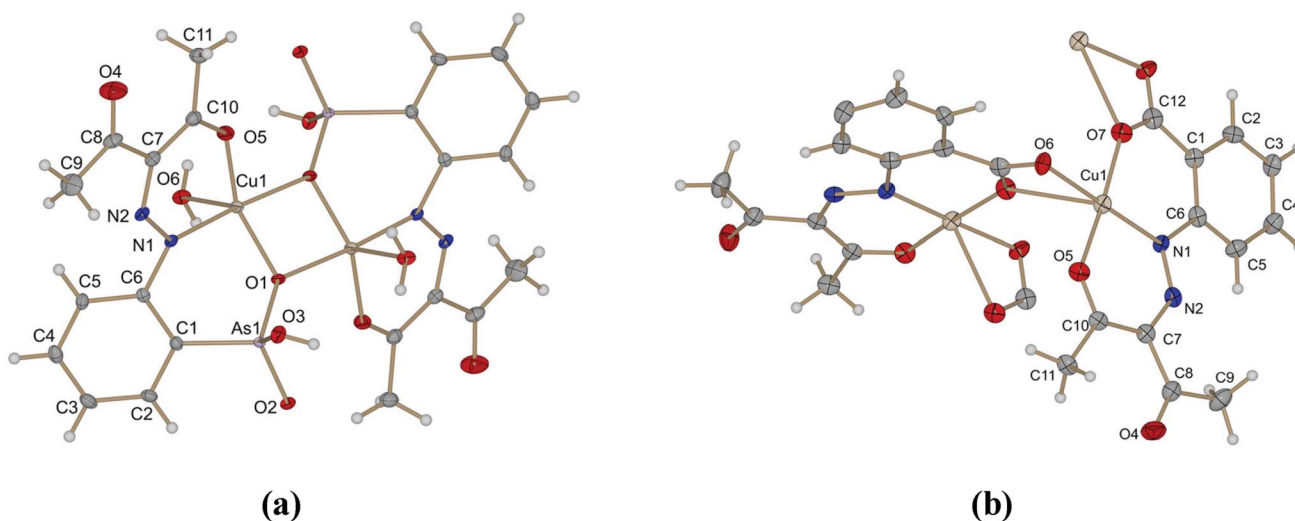


Fig. 3 Thermal ellipsoid plots, drawn at the 50% probability level, of the complexes **9** (a) and **13** (b).

Table 2 Selected structural parameters (distances Å, angles °) of compounds **9–15**

9		10		11		12	
Cu(1)–O(5)	1.900(2)	Cu(1)–O(5)	1.9001(9)	Cu(1)–O(5)	1.959(4)	Cu(1)–O(7)	1.9434(12)
Cu(1)–O(1)	1.9760(19)	Cu(1)–O(1)	1.9560(9)	Cu(1)–N(1)	1.962(5)	Cu(1)–O(6)	1.9644(12)
Cu(1)–N(1)	1.991(2)	Cu(1)–N(1)	1.9616(10)	Cu(1)–O(7)	1.987(5)	Cu(1)–O(5)	2.4489(11)
Cu(1)–O(6)	2.257(2)	Cu(1)–O(7)	1.9908(9)	Cu(1)–O(6)	2.013(5)	N(1)–N(2)	1.3077(19)
Cu(1)–Cu(1)#1	3.109(2)	Cu(1)–O(6)	2.2462(9)	Cu(1)–O(1)	2.308(4)	N(1)–C(6)	1.409(2)
O(5)–C(10)	1.255(3)	O(5)–Cu(1)–O(1)	171.85(4)	O(5)–Cu(1)–N(1)	85.36(18)	N(2)–C(7)	1.316(2)
O(4)–C(8)	1.225(4)	O(5)–Cu(1)–N(1)	89.91(4)	O(5)–Cu(1)–O(7)	87.11(18)	O(5)–C(10)	1.2388(19)
O(5)–Cu(1)–O(1)	157.40(9)	O(1)–Cu(1)–N(1)	95.96(4)	N(1)–Cu(1)–O(7)	172.5(2)	O(4)–C(8)	1.225(2)
O(5)–Cu(1)–N(1)	90.56(9)	O(5)–Cu(1)–O(7)	87.54(4)	O(5)–Cu(1)–O(6)	153.18(17)	O(7)–Cu(1)–O(6)	87.61(5)
O(1)–Cu(1)–N(1)	100.10(8)	O(1)–Cu(1)–O(7)	85.29(4)	N(1)–Cu(1)–O(6)	93.44(19)	O(7)–Cu(1)–O(5)	84.74(4)
O(5)–Cu(1)–O(6)	101.75(8)	N(1)–Cu(1)–O(7)	164.37(4)	O(7)–Cu(1)–O(6)	93.3(2)	O(6)–Cu(1)–O(5)	95.79(4)
O(1)–Cu(1)–O(6)	97.41(8)	O(5)–Cu(1)–O(6)	92.25(4)	O(5)–Cu(1)–O(1)	110.18(15)	N(2)–N(1)–C(6)	118.97(13)
N(1)–Cu(1)–O(6)	93.73(8)	O(1)–Cu(1)–O(6)	93.07(4)	N(1)–Cu(1)–O(1)	90.04(16)	N(1)–N(2)–C(7)	121.63(14)
O(1)–Cu(1)–O(1)#1	77.40(8)	N(1)–Cu(1)–O(6)	92.93(4)	O(7)–Cu(1)–O(1)	92.48(17)	N(1)–H(1 N)⋯O(5)	132.6
Cu(1)–O(1)–Cu(1)#1	102.60(8)	O(7)–Cu(1)–O(6)	102.57(4)	O(6)–Cu(1)–O(1)	96.61(16)	N(1)–H(1 N)⋯O(1)	122.5

13		14		15	
Cu(1)–O(7)	1.875(3)	Cu(1)–N(3)	1.953(2)	Cu(1)–O(5)	1.9192(18)
Cu(1)–O(7)#1	2.426(3)	Cu(1)–O(6)	1.9838(18)	Cu(1)–O(1)	1.9754(17)
Cu(1)–O(5)	1.895(3)	Cu(1)–O(8)	2.3956(19)	Cu(1)–N(3)	1.980(2)
Cu(1)–N(1)	1.951(4)	O(5)–C(10)	1.246(3)	Cu(1)–N(1)	1.984(2)
Cu(1)–O(6)	2.037(3)	O(4)–C(8)	1.227(4)	Cu(1)–O(2)#1	2.2981(18)
O(4)–C(8)	1.227(5)	N(1)–N(2)	1.312(3)	N(2)–C(7)	1.339(3)
O(5)–C(10)	1.248(5)	N(2)–C(7)	1.323(4)	O(4)–C(8)	1.220(3)
O(7)–C(12)	1.275(5)	N(3)–C(12)	1.150(3)	O(5)–C(10)	1.260(3)
N(1)–N(2)	1.300(5)	N(4)–C(12)	1.306(4)	O(1)–Cu(1)–N(1)	91.10(8)
N(1)–C(6)	1.438(6)	N(4)–C(14)	1.350(3)	N(3)–Cu(1)–O(2)#1	92.85(8)
N(2)–C(7)	1.338(6)	N(1)⋯O(5)	2.565(3)	O(1)–Cu(1)–N(3)	91.03(8)
O(7)–Cu(1)–O(5)	171.76(13)	N(3)–Cu(1)–O(6)	90.96(9)	O(1)–Cu(1)–O(2)#1	92.51(7)
O(7)–Cu(1)–N(1)	94.65(13)	N(3)–Cu(1)–O(8)	89.32(8)	O(5)–Cu(1)–N(1)	90.48(8)
O(5)–Cu(1)–N(1)	92.57(14)	O(6)–Cu(1)–O(8)	88.63(7)	O(5)–Cu(1)–N(3)	88.36(8)
O(7)–Cu(1)–O(6)	85.78(12)	N(1)–H(1 N)⋯O(5)	152.6	O(5)–Cu(1)–O(1)	175.54(8)
O(5)–Cu(1)–O(6)	86.85(13)	N(2)–C(7)–C(10)	124.0(3)	O(1)–S(1)–C(1)	104.55(11)

Symmetry transformations used to generate equivalent atoms: #1 $x-1, y, z$ **Table 3** Parameters of thermal decomposition of some copper(II)–ADB complexes

Compound	Temperature interval (K)	Weight loss (%)	DTG peak temperature (K)	A (s ⁻¹)	E_a (kJ mol ⁻¹)	$\Delta^\ddagger H$ (kJ mol ⁻¹)	$\Delta^\ddagger S$ (J K ⁻¹ mol ⁻¹)	$\Delta^\ddagger G$ (kJ mol ⁻¹)
Cu₂(μ-L)₂(CH₃OH)₂^{8c}	470–531	16.6	524	4.6	38.3	34.0	-237	158
	567–608	33.7	601	1.8×10^8	66.9	61.9	-188	175
9	454–499	4.1	465	2.7×10^2	57.6	53.7	-202	148
	499–537	33.3	535	1.7×10^7	102	97.4	-111	157
	590–622	4.7	599	8.2×10^4	7.0	2.0	-310	188
	711–716	3.4	714	83	64.1	58.1	-215	212
10	527–575	16.9	536	2.6×10^5	91.3	86.9	-146	165
13	574–617	37.9	580	5.31×10^5	97.1	92.3	-141	174

O(5)–Cu(1)–N(1) and the N(1)–Cu(1)–O(7) angles are of 92.57(14) and 94.65(13)°, respectively. Also, the external O(7)–Cu(1)–O(6) and the O(5)–Cu(1)–O(6) angles are approximately similar (85.78(12) and 86.85(13)°, respectively). Hence, a constitutional modification by an *ortho*-substituted carboxylic group does markedly affect the conformational solid-state structure inherent in the hydrazone framework, and actually helps to stabilize the 1D geometry of the molecule by additional coordination, as well as its supramolecular lattice structure (Fig. S4e†). In accordance with the structure, the coordination polymer **13** is thermally more stable than **9**, decomposing in one step at 574–617 K (Fig. S3d,† Table 3).

The reaction of copper(II) with **4** in water at pH 6 and 393 K allowed the preparation of the mononuclear ADB complex [CuL⁴(H₂O)₂]-H₂O (**10**) (Scheme 6, Route I), which crystallized directly from the reaction mixture as cubic deep green crystals. Analytical data support the formulation and X-ray crystallography (Fig. 4a) shows a distorted trigonal-bipyramidal coordination, with two positions being occupied by the O(6) and O(7) oxygen atoms of water molecules. The presence of the *ortho*-substituent at the aromatic ring creates one more six-membered metallacycle with copper(II). On the other hand, steric effects caused by the coordinated water molecules lead to anomalous Cu–O distances of Cu–O(6) (2.2462(9) Å) and Cu–O(7) (1.9908(9) Å). The

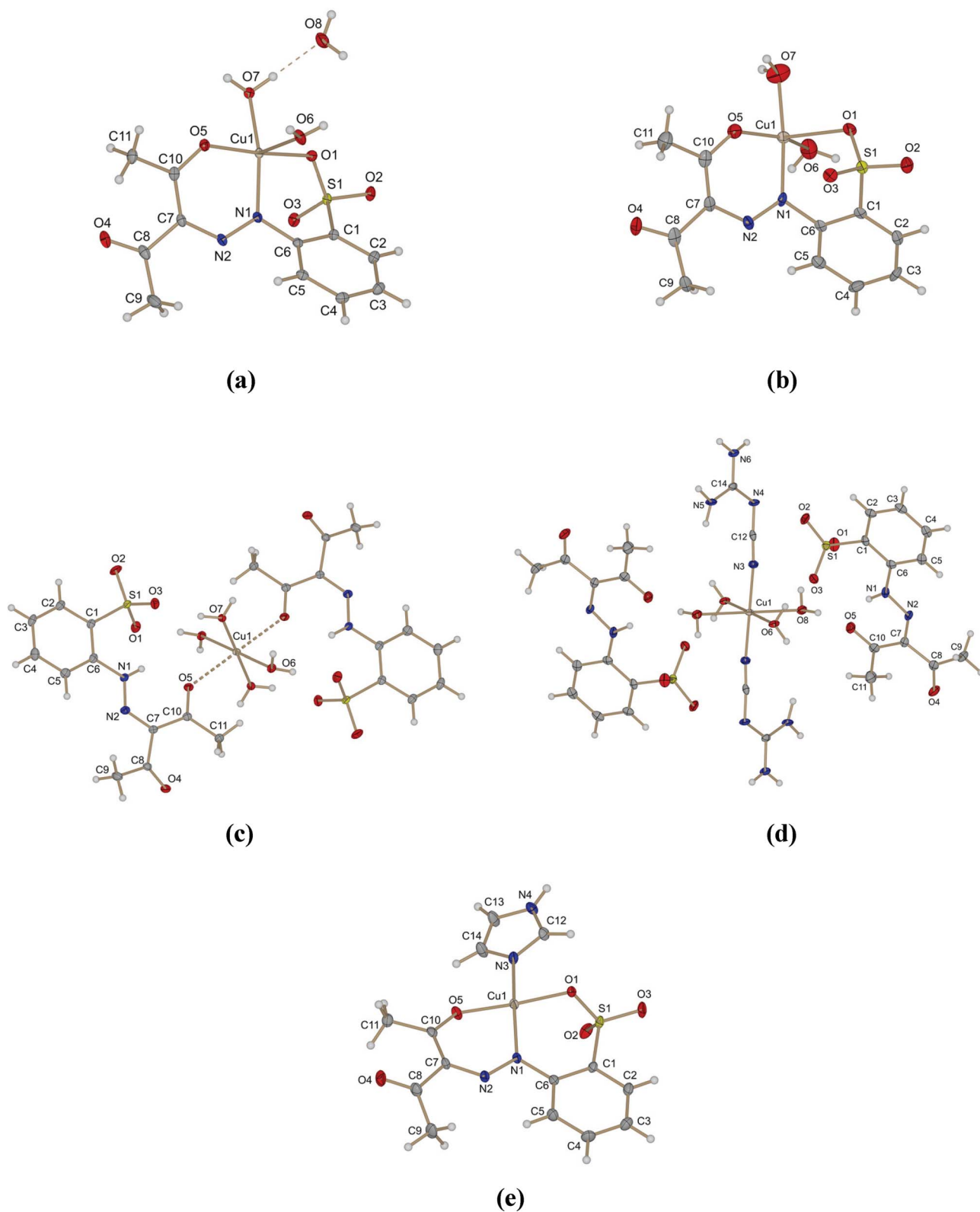
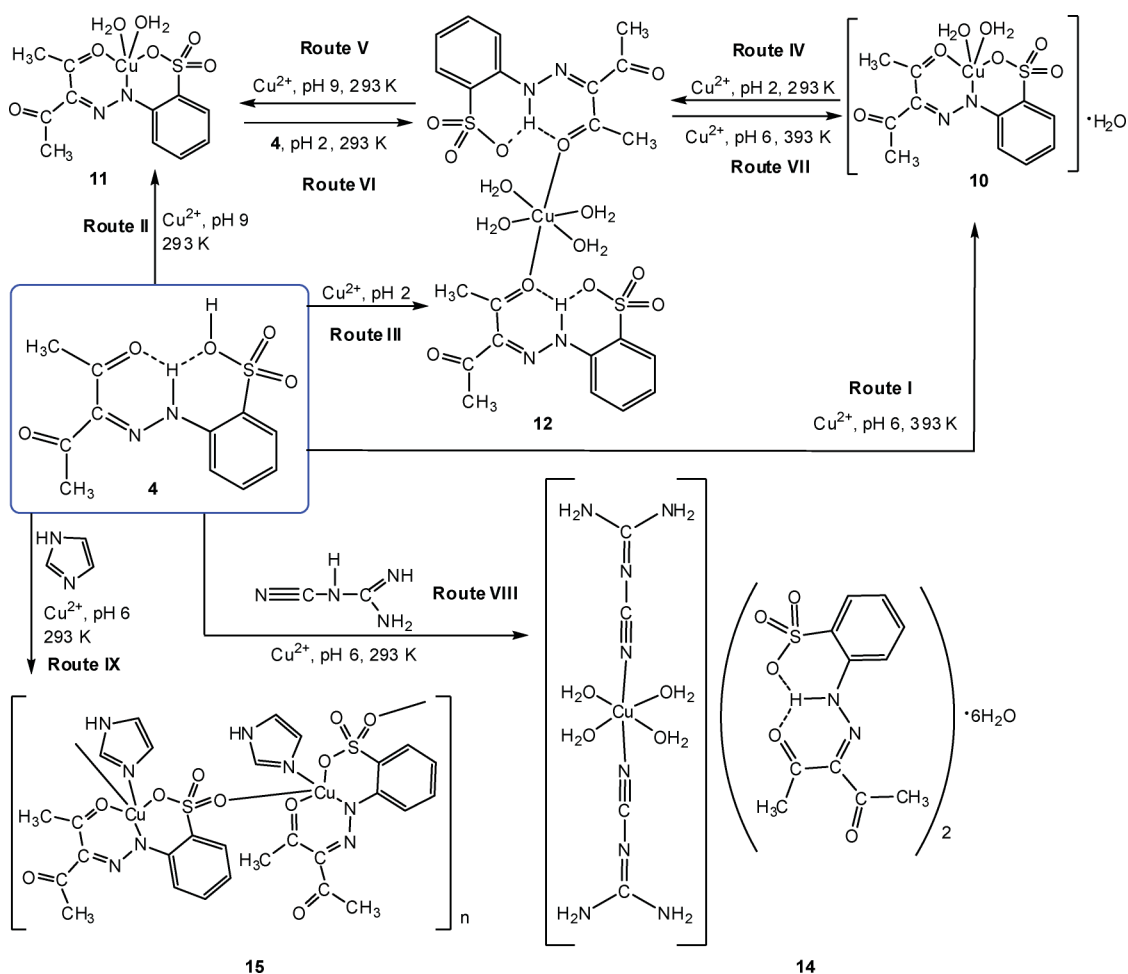


Fig. 4 Thermal ellipsoid plots, drawn at the 50% probability level of the complexes **10** (a), **11** (b), **12** (c), **14** (d) and **15** (e). In **15** the imidazole ring was disordered over two sites. The disorder was omitted from the drawing.



Scheme 6

six-membered chelate rings exhibit a slightly distorted half chair conformation with the copper atom laying outside the plane defined by the pentane-2,4-dione moiety. The aromatic rings of the ligands adopt an angle of 58.8° with reference to the basal plane of the coordination polyhedron. The crystal packing of the complex is characterized by layers of molecules extending in parallel to the crystallographic a plane. The overall layer structure (Fig. S4b†) can be regarded as a two dimensional coordination polymer in which the molecules are nested in such a way that a close packing results. As all of the strong acceptors are involved in the complexation, only weak aromatic π -interactions between the sulfo residues (plane-plane distance of 4.7 \AA) of consecutive layers exist. Under heating, complex **10** decomposes in one step, which occurs in the $527\text{--}575 \text{ K}$ range (Table 3, Fig. S3c†) with a strong and sharp DTG peak at 536 K , indicating a rapid and vigorous decomposition with activation energy of 91.3 kJ mol^{-1} and a negative $\Delta^\ddagger S$ value.

Curiously, if the reaction of copper(II) with **4** is performed at pH 9 (NH_4OH) and at room temperature, the greenish-black compound $[\text{CuL}^4(\text{H}_2\text{O})_2]$ **11** (related to **10** but without crystallization water) is formed (Scheme 6, Route II), while at pH 2 (HCl) the reaction gives another di-ADB monomeric complex, $[\text{Cu}(\text{HL}^4)_2(\text{H}_2\text{O})_4]$ **12** (Scheme 6, Route III). In the structure of **11** (Fig. 4b), similarly to **10**, the coordination positions of the

copper(II) are occupied by one carbonyl oxygen, one hydrazone nitrogen, one oxygen of a sulfo group and the oxygens of two water molecules, and two six-membered metallacycles are formed. The $\text{Cu}(1)\text{--O}(5)$ distance ($1.959(4) \text{ \AA}$) is shorter than the $\text{Cu}(1)\text{--O}(1)$ one ($2.308(4) \text{ \AA}$), while the $\text{C}(10)\text{=O}(5)$ distance ($1.256(7) \text{ \AA}$) is longer than $\text{C}(8)\text{=O}(4)$ ($1.244(7) \text{ \AA}$) due to the coordination of the former moiety to copper. Comparison of the $\text{O}(5)\text{--Cu}(1)\text{--O}(1)$ angles in **11** and **10** shows a dramatic increase from $110.18(15)^\circ$ to $171.85(4)^\circ$ due to the interaction with hydrate water in the latter compound. A regular geometric configuration was found, with $\text{N}(1)\text{--Cu}(1)\text{--O}(6)$, $\text{O}(7)\text{--Cu}(1)\text{--O}(6)$, $\text{N}(1)\text{--Cu}(1)\text{--O}(1)$, $\text{O}(7)\text{--Cu}(1)\text{--O}(1)$ and $\text{O}(6)\text{--Cu}(1)\text{--O}(1)$ angles of $93.44(19)$, $93.3(2)$, $90.04(16)$, $92.48(17)$ and $96.61(16)^\circ$, respectively. The crystal structure of **11** is stabilized by strong hydrogen bond interactions *via* coordinated water molecules and the uncoordinated carbonyl group (Fig. S4c†).

The bulky light greenish-yellow crystals of **12** are of the monoclinic space group $\text{P}2_1/\text{n}$. The $\text{Cu}(\text{H}_2\text{O})_4^{2+}$ unit bridges two unideprotonated (SO_3^-) ligand molecules (Scheme 6, Fig. 3) which coordinate *via* carbonyl groups and do not chelate to copper(II) since the RAHB H-bond systems $\text{N}(1)\text{--N}(1\text{H})\text{--O}(5)$ and $\text{N}(1)\text{--N}(1\text{H})\text{--O}(1)$ (Scheme 4) remain intact. The $\text{N}(1)\text{--O}(5)$ and $\text{N}(1)\text{--O}(1)$ distances are $2.6235(18)$ and $2.9513(18) \text{ \AA}$, respectively in two six-membered hydrogen bonded cycles. The

positive charges of the copper(II) are neutralized by the negative charges of the sulfo groups. The Cu(1)–O(6) (1.9644(12) Å) and Cu(1)–O(7) (1.9434(12) Å) distances are shorter than the Cu(1)–O(5) distance (2.4489(11) Å), possibly due to steric hindrance of the coordinated water molecules. The overall crystal structure is stabilized by strong hydrogen bonding interactions between the coordinated water hydrogens and both the sulfo- and ketone groups in adjacent units (Fig. S4d†). Curiously, at pH 2, even at elevated temperatures (393 K), the reaction of copper(II) with **4** gives only **12**, indicating that for the destruction of the RAHB system one has to use an alkali medium.

Apart from the above described reactions, the interconversions between **12**, **11** and **10** (Scheme 6, Routes IV–VII) were also confirmed (see Experimental). Thus, the conversion of the diligand monomer **12** to the monoligand monomers **10** and **11** or *vice versa* was found to be pH and temperature dependent. These factors are essential for the destruction of the RAHB system, allowing the copper(II) ions to enter the ONO chelating pocket of the ligand. This idea can be extended further by addition of an extra ligand other than ADB. Thus, when **4** and cyanoguanidine are added simultaneously to a copper(II) solution at pH 6 and room temperature, **4** does not coordinate to copper(II) keeping its RAHB intact and only cyanoguanidine binds to the metal through its cyano group yielding $[\text{Cu}(\text{H}_2\text{O})_4\{\text{NCNC}(\text{NH}_2)_2\}_2](\text{HL}^4)_2 \cdot 6\text{H}_2\text{O}$ **14** (Scheme 6, Route VIII). In **14**, the positive charges of copper(II) are compensated by the negative charges of two sulfonate groups of the deprotonated **4**. The H-bond found in the RAHB N(1)–H(1 N) \cdots O(5), with a N \cdots O distance of 2.565(3) Å, falls within the N \cdots O 2.50–2.62 Å distance range observed in previous studies on ADBs.^{6,8,12,13} Due to the hydrogen bonding involving O(5), the C(10)–O(5) bond length is longer than that of uncoordinated C(8)–O(4) (1.246(3) Å and 1.227(4) Å, respectively). The coordination sphere of copper(II) is formed by four coordinated water molecules and two cyanoguanidines. The C(12)–N(4) distance (1.306(4) Å) is shorter than the N(4)–C(14) distance (1.350(3) Å) due to the π -delocalization along N(6)[or N(5)]–C(14)=N(4)–C(12) \equiv N(3) \rightarrow Cu. The angles around copper(II), N(3)–Cu(1)–O(6), N(3)–Cu(1)–O(8) and O(6)–Cu(1)–O(8), are 90.96(9)°, 89.32(8)° and 88.63(7)°, respectively.

Another situation is observed when copper(II) reacts with **4** in the presence of imidazole (im). This facilitates the destruction of the RAHB, copper(II) enters into the chelating ONO pocket of **4** and the coordination polymer $[\text{Cu}(\mu\text{-L}^4)(\text{im})]_n$ **15**, with

pentacoordinated copper(II), is formed (Scheme 6, Route IX). The coordination of one oxygen atom of each sulfo group (Cu(1)–O(2)#1 distance of 2.2981(18) Å) is involved in the polymer formation; the O(1)–Cu(1)–O(2)#1 and N(3)–Cu(1)–O(2)#1 angles are 92.51(7)° and 92.85(8)°, respectively (Fig. 4e). The imidazole is coordinated perpendicularly to the O(1)–Cu(1)–O(5) plane with O(1)–Cu(1)–N(3) and N(3)–Cu(1)–O(5) angles of 91.03(8)° and 88.36(8)°, respectively. The metal pertains to two different six-membered metallacycles, Cu(1)–O(1)–S(1)–C(1)–C(6)–N(1) and Cu(1)–O(5)–C(10)–C(7)–N(2)–N(1), with O(5)–Cu(1)–N(1) and O(1)–Cu(1)–N(1) angles of 90.48(8)° and 91.10(8)°, respectively. The C(10)–O(5) distance is larger than for the uncoordinated carbonyl C(8)–O(4) (1.260(3) and 1.220(3) Å, respectively), due to the coordination of O(5). The packing of **15** is stabilized *via* strong intermolecular interactions (Fig. S4g†).

To estimate the relative stability of the various types of complexes, theoretical calculations of the model species $[\text{Cu}(\text{OH})(\text{L}^8)(\text{H}_2\text{O})] \cdot \text{H}_2\text{O}$, $[\text{Cu}(\text{L}^1)(\text{H}_2\text{O})_2] \cdot \text{H}_2\text{O}$ and $[\text{Cu}(\text{L}^4)(\text{H}_2\text{O})_2] \cdot \text{H}_2\text{O}$ (Scheme 7) were performed. The calculations indicate that the negative ΔG_s value of the formation of $[\text{Cu}(\text{L}^4)(\text{H}_2\text{O})_2] \cdot \text{H}_2\text{O}$ bearing two fused six-membered metallacycles is the highest ($-37.5 \text{ kcal mol}^{-1}$, see computational details). The formation of $[\text{Cu}(\text{L}^1)(\text{H}_2\text{O})_2] \cdot \text{H}_2\text{O}$ is less exoergonic ($\Delta G_s = -24.0 \text{ kcal mol}^{-1}$) indicating a lower stability of the five-membered cycle compared to the six-membered one. $[\text{Cu}(\text{OH})(\text{L}^8)(\text{H}_2\text{O})] \cdot \text{H}_2\text{O}$ is the least stable complex (the ΔG_s of formation is $-7.7 \text{ kcal mol}^{-1}$) due to the presence of only one metallacycle in its structure.

The redox properties of $[\text{Cu}_2(\mu\text{-L}^1)_2(\text{CH}_3\text{OH})_2]^{8e}$ **9**, **10** and **13** have been investigated by cyclic voltammetry, at a Pt disk electrode, in a 0.2 M $[\text{Bu}_4\text{N}][\text{BF}_4]/\text{NCMe}$ or DMSO solution, at room temperature. Complexes $[\text{Cu}_2(\mu\text{-L}^1)_2(\text{CH}_3\text{OH})_2]$ and **10** exhibit two single-electron (per metal atom) irreversible reduction waves (Fig. 5), assigned to the $\text{Cu}^{\text{II}} \rightarrow \text{Cu}^{\text{I}}$ (wave I) and $\text{Cu}^{\text{I}} \rightarrow \text{Cu}^{\text{0}}$ (wave II) reductions, at the reduction peak potential values given in Table 4 (${}^{\text{I}}E_{\text{p}/2}^{\text{red}}$ in the range -0.44 to -0.05 V vs. SCE , and ${}^{\text{II}}E_{\text{p}/2}^{\text{red}}$ between -1.08 and -1.48 V vs. SCE). In addition, a new irreversible anodic wave (wave *a*), at *ca.* -0.15 V vs. SCE is observed upon scan reversal after the first reduction wave. It plausibly corresponds to the oxidation of the Cu^{I} species formed at the first reduction process. The sharp shape of the wave indicates that such a Cu^{I} species is adsorbed at the electrode surface.

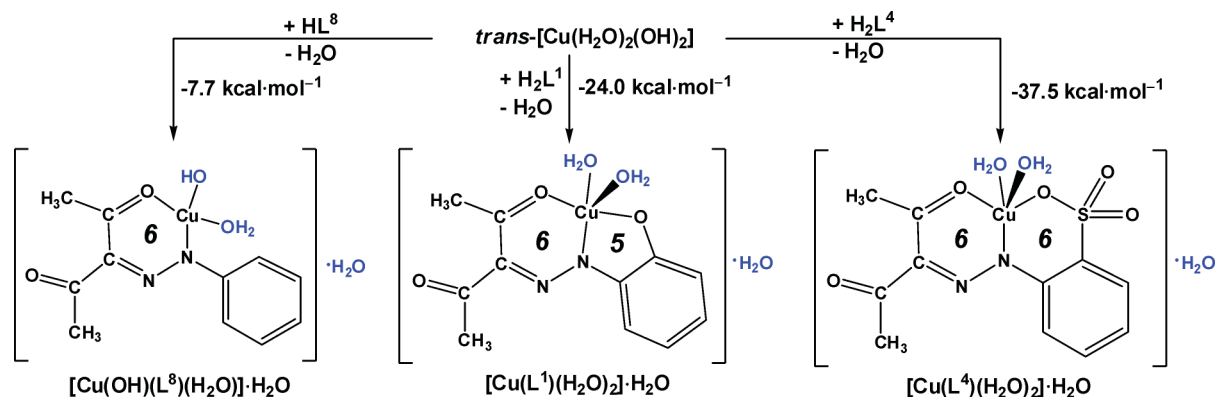


Table 4 Cyclic voltammetric data^a for some copper(II) complexes with ADB

Complexes	X	¹ E _{p/2} ^{red}	^{II} E _{p/2} ^{red}	¹ E _{p/2} ^{ox}	E _p ^{oxb}
[Cu ₂ (μ-L) ₂ (CH ₃ OH) ₂]	OH	-0.44	-1.08	1.16	-0.15
10	SO ₃ H	-0.05	-1.48	1.26	-0.17
13	COOH	-0.96	—	1.11	—

^a Values given in V ± 0.02 relative to the SCE, scan rate = 0.2 V s⁻¹. ^b Anodic wave (a) generated upon scan reversal following the first reduction wave.

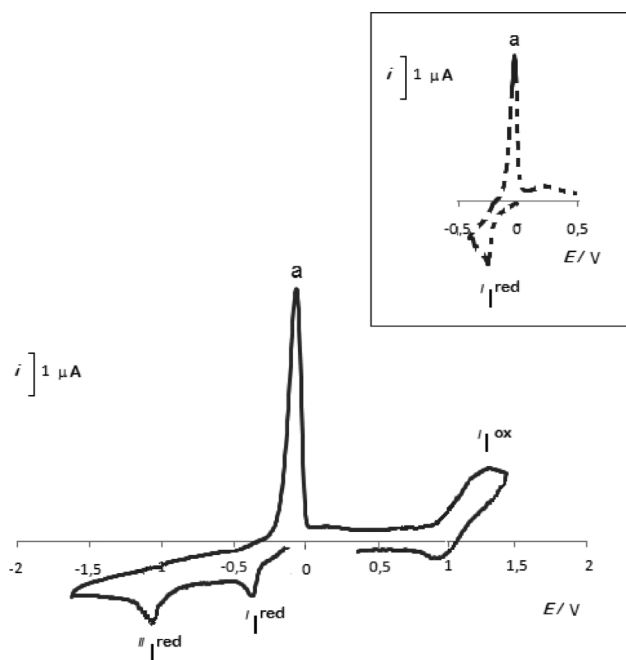


Fig. 5 Cyclic voltammogram ($\nu = 0.2 \text{ V s}^{-1}$) of a 1.7 mM solution of [Cu₂(μ-L)₂(CH₃OH)₂], initiated by the cathodic sweep, in 0.2 M [tBu₄N][BF₄]/NCMe, at a platinum disk electrode ($d = 0.5 \text{ mm}$).

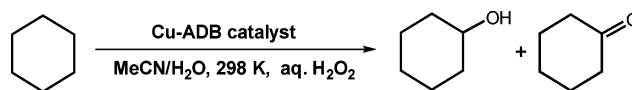
The occurrence of a single-electron reduction per Cu^{II} (or Cu^I) ion has been confirmed by exhaustive controlled potential electrolysis (CPE) at a potential slightly cathodic to that of the peak potentials of wave I (or II). CPE at any of the reduction waves corresponds to a charge consumption of 1 F mole⁻¹ of complex for **10** or 2 F mole⁻¹ of complex for the dinuclear [Cu₂(μ-L)₂(CH₃OH)₂] compound. The cathodically generated Cu^I species appear to be stable in the solvent/electrolyte medium along the CPE since the corresponding Cu^{I/II} oxidation wave is observed at the end of the electrolysis (Table 4). The CPE performed at the second reduction wave leads to the deposition of metallic copper. Moreover, for the dinuclear complex [Cu₂(μ-L)₂(CH₃OH)₂] no metal–metal electronic interaction has been detected, since any of the cathodic waves involves the reduction of the two metal ions, without differentiation of distinct waves at different potentials. For complex **13**, only one irreversible reduction wave was observed at -0.96 V vs. SCE involving 2e per metal ion as indicated by CPE.

The compounds show irreversible or partially reversible oxidation waves at ca. 1.2 V (Fig. 5 for complex [Cu₂(μ-L)₂(CH₃OH)₂]) which can involve the 3-(*ortho*-substituted phenylhydrazo)pentane-2,4-dione ligands (when uncoordinated, they undergo irreversible oxidations at comparable potentials, e.g. at E_{p/2}^{ox} 1.23, 1.36 V and 1.61 vs. SCE for X = OH, SO₃H or

COOH, respectively, see Table 1) and were not investigated further. Apparently, there are not any correlations between Hammett's and related substituents constant and the oxidation or reduction potentials. In the case of **9**, no wave has been observed under the experimental conditions of this study.

Catalytic activity of the copper complexes

Complexes **9**, **10**, **12** and **13** act as catalysts or catalyst precursors for the oxidation of cyclohexane, in acetonitrile, to a cyclohexanol and cyclohexanone mixture, by aqueous hydrogen peroxide in acidic medium at room temperature (Scheme 8) with a total yield of ca. 20% and turnover number (TON) values up to 566 moles of products per mole of catalyst, for a single batch (Table 5). Control reactions carried out in the absence of the metal complex catalyst and with or without the free ligands **2**, **4** and **6** (entries 8 and 9), indicate that no cyclohexane oxidation reaction then occurs, while the use of Cu(NO₃)₂ (entry 10) leads to an overall yield of only 5%.



Scheme 8

The higher activity of **12** may be accounted for by the presence of the four labile water ligands and lower steric hindrance around the metal centre. The activities of **9** and **13** (dimer and polymer, respectively) are similar under standard conditions (product yields ca. 16%, Table 5, entries 1 and 4), slightly higher than that of the mononuclear complex **10** (entry 2) and lower than that of [Cu₂(μ-L)₂(CH₃OH)₂]^{8c} (entry 7). Dinuclear copper peroxo complexes can be involved in those types of reactions,^{15,16,17a} and the dimer **9** and polymer **13** bear relatively close copper(II) atoms supported by ADB bridging ligands, that can assist the formation of such a type of peroxo species.

It is known that the peroxidative oxidation of cyclohexane catalyzed by copper(II) complexes usually proceeds more efficiently in an acidic medium.¹⁷ Accordingly, the addition of an acid promoter

Table 5 Peroxidative oxidation of cyclohexane to cyclohexanol and cyclohexanone^a

Entry	Catalyst	Yield ^b of products, %			TON ^d
		Alcohol	Ketone	Total ^c	
1	9 ^e	6.9	9.9	16.8	34.2
2	10 ^e	4.3	7.1	11.4	11.4
3	12 ^e	9.3	10.9	20.2	35.5
4	13 ^e	7.2	9.1	16.3	16.7
5	10 ^f	4.4	7.0	11.4	326
6	12 ^f	8.9	10.9	19.8	566
7	[Cu ₂ (μ-L) ₂ (CH ₃ OH) ₂]	7.1	16.6	23.7	23.7
8	—	—	—	— ^g	—
9	2, 4 or 6	—	—	— ^g	—
10	Cu(NO ₃) ₂	1.6	3.8	5.4	5.4

^a Selected data; reaction conditions: C₆H₁₂ (1 mmol), Cu-catalyst (see footnotes ^e and ^f), MeCN/H₂O 4 mL, *n*(HNO₃)/*n*(Cat) = 10, H₂O₂ (10 mmol added as an aqueous 30% solution), 6 h reaction time, 298 K; ^b Moles of product/100 moles of C₆H₁₂ (Alcohol = cyclohexanol, Ketone = cyclohexanone); ^c Cyclohexanol + cyclohexanone; ^d Overall TON values (moles of products/mole of catalyst); ^e 4.9–10.0 μmol; ^f 0.35 μmol; ^g Traces, < 0.3%.

(typically HNO₃) leads to higher activities for both **10** and **12**, which achieve the optimum values for the acid-to-catalyst molar ratio of *ca.* 10:1 (Table S4 and Fig. S5†). A further increase in the acid additive amount (acid-to-catalyst molar ratio within the 10–60 range) does not result in a higher activity in the case of **10** and even lowers the performance of **12**. However, for **9** and **13**, the presence of acid does not appreciably affect the product yields, which remain practically constant in the $n(\text{HNO}_3)/n(\text{catalyst})$ range of 0–60 (Fig. S5†). Although the role of the acid co-catalyst remains not fully established, it presumably can be associated with the resulting unsaturation of the metal centre upon ligand protonation, the enhancement of the oxidative properties of the metal catalyst, and the hampering of the decomposition of H₂O₂ to water and oxygen.¹⁷

Other important factors in the performance of the system concern the relative amounts of oxidant (hydrogen peroxide) and catalyst. An increase in the peroxide-to-catalyst molar ratio results in a yield enhancement (Fig. S6†), *e.g.* from 7–10 to 12–22% upon changing that ratio from 500 to 1250 (H₂O₂ amount increase from 5.0 to 12.5 mmol). A decrease of the catalyst amount below the typical value of 5–10 μmol results in comparable yields and in enhancements of the overall TON *e.g.* from 11 or 36 up to 326 or 566, for complex **10** or **12**, respectively (Table 5, entries 2,3,5,6).

The cyclohexane oxidation appears to proceed mainly *via* radical mechanisms involving both carbon-centred and oxygen-centred radicals in view of the pronounced decrease (by *ca.* 88–70%) of the catalytic activity when the experiments are performed in the presence of either a carbon radical trap (*e.g.*, CBrCl₃) or an oxygen radical trap (*e.g.*, Ph₂NH).^{17d} Hence, although the detailed mechanistic pathway is still to be established, it can possibly proceed, as suggested in other cases,^{10,17,18} through H-abstraction from cyclohexane, conceivably by the hydroxyl radical HO• (formed by metal-assisted decomposition of H₂O₂) to form the cyclohexyl radical Cy•. Reaction of Cy• with O₂ gives the organoperoxy CyOO•, or with a metal-hydroperoxy species yields cyclohexyl hydroperoxide (CyOOH) which can also be formed upon H-abstraction from H₂O₂ (or derived HOO•) by CyOO•.^{10c-e,17a,e-h,18i} The organohydroperoxide CyOOH can undergo metal-assisted decomposition to alkoxy (CyO•, upon O–O bond cleavage) and alkylperoxy (CyOO•, upon O–H bond rupture) radicals from which the final oxygenates can be formed.^{10c-e,17a,c,18a,e-h} The involvement of CyOOH is recognized by the increase in the amount of CyOH with the corresponding decrease of the cycloketone upon treatment of the final reaction solution with an excess of PPh₃ prior to the GC analysis, following the method reported by Shul'pin.^{18a,b,f}

In summary, the overall yields up to *ca.* 20% in a single batch achieved in this work are comparable with those obtained by other valuable copper and iron based catalysts¹⁸ and are higher than those achieved with half-sandwich scorpionate tris(pyrazolyl)methane complexes of vanadium, iron or copper,¹⁹ as well as other Cu catalytic systems namely with salen or phthalocyanine ligands,²⁰ although not reaching those reported for a few remarkably active multicopper triethanolamine complexes.^{10a,17b}

Conclusions

The functional groups X in 3-(*ortho*-substituted phenylhydrazo)pentane-2,4-diones, X-2-C₆H₄-NHN=C{C(=O)CH₃}₂,

influence their coordination and other properties (*e.g.* δ_{N-H} and redox potentials) and, depending on X and on the reaction conditions with copper(II), different metal–ADB monomers, dimers and polymers are formed. The versatility of those compounds as ligands is well illustrated by the tunable synthesis of the variety of complexes we have prepared herein with different geometries and nuclearities. By taking advantage of the coordination ability of the *ortho*-substituent of ADB, particularly stable complexes with two fused six-membered metallacycles can be synthesized.

The study also shows that the Cu–ADB complexes act as efficient and selective catalysts for the peroxidative oxidation of cyclohexane to the corresponding alcohol and ketone in aqueous MeCN medium, the ADB thus behaving as quite adequate ligands for such metal catalyzed reactions. Their use deserves to be further explored for other types of oxidation catalysis and/or other metals.

Experimental

Materials and instrumentation

The ¹H and ¹³C NMR spectra were recorded at room temperature on a Bruker Avance II + 300 (UltraShield™ Magnet) spectrometer operating at 300.130 and 75.468 MHz for proton and carbon-13, respectively. The chemical shifts are reported in ppm using tetramethylsilane as the internal reference. The infrared spectra (4000–400 cm⁻¹) was recorded on a BIO-RAD FTS 3000MX instrument in KBr pellets. Carbon, hydrogen, and nitrogen elemental analyses were carried out by the Microanalytical Service of the Instituto Superior Técnico. All of the synthetic work was performed in air and at room temperature. Thermal properties were analyzed with a Perkin–Elmer Instruction system (STA6000) at a heating rate of 10 K min⁻¹ under a dinitrogen atmosphere. Electrospray mass spectra were run with an ion-trap instrument (Varian 500-MS LC Ion Trap Mass Spectrometer) equipped with an electrospray (ESI) ion source. For electrospray ionization, the drying gas and flow rate were optimized according to the particular sample with 35 p.s.i. nebulizer pressure. Scanning was performed from *m/z* 100 to 1200 in methanol solution. The compounds were observed in the positive mode (capillary voltage = 80–105 V). Chromatographic analyses were undertaken by using a Fisons Instruments GC 8000 series gas chromatograph with a DB-624 (J&W) capillary column (FID detector) and the Jasco–Borwin v.1.50 software. The internal standard method was used to quantify the organic products. The electrochemical experiments were performed on an EG&G PAR 273A potentiostat/galvanostat connected to a personal computer through a GPIB interface. Cyclic voltammetry (CV) studies were undertaken at room temperature using a two-compartment three-electrode cell with a Pt disc working (*d* = 0.5 mm) and a Pt wire counter electrode. Controlled-potential electrolyses (CPE) were carried out in a three-electrode H-type cell. The compartments were separated by a sintered glass frit and equipped with platinum gauze working and counter electrodes. For both CV and CPE experiments, a Luggin capillary connected to a silver wire pseudo-reference electrode was used to control the working electrode potential, and a Pt wire was employed as the counter-electrode for the CV cell. The CPE experiments were monitored regularly by cyclic voltammetry, thus assuring no significant potential drift occurred along the electrolyses. The solutions were saturated with dinitrogen by bubbling through this gas before each run. The

redox potentials of the compounds were measured in 0.2 M [t -Bu₄N][BF₄]/NCMe or DMSO, using ferrocene as an internal reference and all reported potentials are quoted relative to the SCE by using the [Fe(η^5 -C₅H₅)₂]^{0/+} redox couple ($E_{1/2}^{ox} = 0.42$ or 0.44 V vs. SCE in NCMe or DMSO, respectively).²¹

Syntheses of 3-(2-substituted phenylhydrazo)pentane-2,4-diones (1–8)

The syntheses and some characteristics of **1** and **6–8** were reported earlier;^{8c,12} the arylhydrazones **2–5** were synthesized *via* a modified¹³ Japp–Klingemann reaction^{1–3} between the aromatic diazonium salt of 2-substituted aniline and pentane-2,4-dione in water solution containing sodium hydroxide.

Diazotization. 2-Substituted aniline (25 mmol) was dissolved in 50 mL water, and 0.5 g (12.5 mmol) of NaOH was added. The solution was cooled in an ice bath to 273 K and 1.725 g (25 mmol) of NaNO₂ were added; 5.00 mL HCl were then added in 0.5 mL portions for 1 h. The temperature of the mixture should not exceed 278 K.

Azocoupling. NaOH (1.00 g, 25 mmol) was added to a mixture of 2.55 mL (25 mmol) of pentane-2,4-dione with 50 mL of water. The solution was cooled in an ice bath to *ca.* 273 K, and a suspension of 2-substituted aniline diazonium (see above) was added in three portions under vigorous stirring for 1 h.

HL¹ (1). Yield: 72% (based on pentane-2,4-dione), black powder soluble in methanol, ethanol, acetone and insoluble in water and chloroform. Anal. Calcd for C₁₁H₁₂N₂O₃ ($M = 220$): C, 60.00 (calc. 59.88); H, 5.45 (5.47); N, 12.73 (12.20)%. IR (KBr): 3468 ν (OH), 3079 ν (NH), 1668 ν (C=O), 1632 ν (C=O...H), 1599 ν (C=N) cm⁻¹. ¹H-NMR (300.130 MHz) in DMSO, internal TMS, δ (ppm): 2.41 (s, 3H, CH₃), 2.48 (s, 3H, CH₃), 6.91–7.67 (4H, Ar–H), 10.51 (s, 1H, OH), 14.58 (s, 1H, NH). ¹³C-¹H} NMR (75.468 MHz) in DMSO, internal TMS, δ (ppm): 26.5 (CH₃), 31.2 (CH₃), 114.9 (Ar–H), 115.8 (Ar–H), 120.2 (Ar–H), 126.2 (Ar–H), 129.3 (Ar–NH–N), 133.2 (C=N), 146.3 (Ar–OH), 196.2 (C=O), 196.4 (C=O).

HL² (2). Yield 67% (based on pentane-2,4-dione), yellow powder soluble in DMSO, water and insoluble in methanol, ethanol and acetone. Elemental analysis: C₁₁H₁₃AsN₂O₅ ($M = 328.15$); C 40.13 (calc. 40.26); H 4.58 (4.49); N 8.39 (8.54)%. IR (KBr): 3400 ν (OH), 3069 ν (NH), 1674 ν (C=O), 1644 ν (C=O...H), 1575 ν (C=N) cm⁻¹. ¹H-NMR (300.130 MHz) in DMSO, internal TMS, δ (ppm): 2.27 (s, 3H, CH₃), 2.72 (s, 3H, CH₃), 6.75–7.71 (m, 4H, Ar–H), 14.05 (s, 1H, N–H). ¹³C-¹H} NMR (75.468 MHz) in DMSO, internal TMS, δ (ppm): 27.64 (CH₃), 32.22 (CH₃), 118.99 (Ar–H), 123.53 (Ar–H), 127.33 (Ar–NH–N), 133.13 (Ar–H), 135.63 (Ar–H), 136.24 (C=N), 144.94 (Ar–AsO₃H₂), 199.80 (C=O), 202.90 (C=O).

HL³ (3). Yield 72% (based on pentane-2,4-dione), yellow powder soluble in DMSO, methanol, ethanol and acetone, and insoluble in water. Elemental analysis: C₁₁H₁₁Cl₁N₂O₂ ($M = 238.67$); C 55.29 (calc. 55.36); H 4.65 (4.55); N 11.79 (11.74)%. IR (KBr): 3436 ν (NH), 1669 ν (C=O), 1636 ν (C=O...H), 1588 ν (C=N) cm⁻¹. ¹H-NMR (300.130 MHz) in DMSO, internal TMS, δ (ppm): 2.07 (s, 3H, CH₃), 2.43 (s, 3H, CH₃), 7.19–7.85 (m, 4H, Ar–H), 14.53 (s, 1H, N–H). ¹³C-¹H} NMR (75.468 MHz) in DMSO, internal TMS, δ (ppm): 26.49 (CH₃), 31.25 (CH₃), 116.21

(Ar–H), 120.47 (Ar–H), 126.09 (Ar–H), 128.84 (Ar–Cl), 129.82 (Ar–H), 134.58 (C=N), 137.81 (Ar–NH–N), 196.31 (C=O), 197.47 (C=O).

HL⁴ (4). Yield 75% (based on pentane-2,4-dione), yellow powder soluble in DMSO, water and insoluble in methanol, ethanol and acetone. Elemental analysis: C₁₁H₁₂N₂O₅S ($M = 284.29$); C 45.33 (calc. 46.47); H 4.18 (4.25); N 9.79 (9.85)%. IR (KBr): 3447 ν (NH), 1676 ν (C=O), 1641 ν (C=O...H), 1578 ν (C=N) cm⁻¹. ¹H-NMR (300.130 MHz) in DMSO, internal TMS, δ (ppm): 1.68 (s, 3H, CH₃), 2.44 (s, 3H, CH₃), 7.14–7.82 (m, 4H, Ar–H), 14.71 (s, 1H, N–H). ¹³C-¹H} NMR (75.468 MHz) in DMSO, internal TMS, δ (ppm): 26.58 (CH₃), 31.07 (CH₃), 115.77 (Ar–H), 124.16 (Ar–H), 127.46 (Ar–H), 130.44 (Ar–H), 133.83 (C=N), 135.42 (Ar–SO₃H), 138.50 (Ar–NH–N), 194.96 (C=O), 196.76 (C=O).

HL⁵ (5). Yield 66% (based on pentane-2,4-dione), yellow powder soluble in DMSO, methanol, ethanol and acetone, and insoluble in water. Elemental analysis: C₁₃H₁₄N₂O₄ ($M = 262.26$); C 59.42 (calc. 59.54); H 5.29 (5.38); N 10.57 (10.68)%. IR (KBr): 3449 ν (NH), 1701 ν (C=O), 1669 ν (C=O), 1646 ν (C=O...H), 1601 ν (C=N) cm⁻¹. ¹H-NMR (300.130 MHz) in DMSO, internal TMS, δ (ppm): 2.46 (s, 3H, CH₃), 2.50 (s, 3H, CH₃), 3.94 (s, 3H, CH₃), 7.25–8.04 (m, 4H, Ar–H), 15.08 (s, 1H, N–H). ¹³C-¹H} NMR (75.468 MHz) in DMSO, internal TMS, δ (ppm): 26.52 (CH₃), 31.16 (CH₃), 52.52 (CH₃), 115.13 (Ar–CC=O), 115.64 (Ar–H), 124.11 (Ar–H), 131.05 (Ar–H), 134.86 (Ar–H), 134.94 (C=N), 143.21 (Ar–NH–N), 166.18 (C=O), 195.97 (C=O), 196.70 (C=O).

HL⁶ (6). Yield 81% (based on pentane-2,4-dione), yellow powder soluble in DMSO, methanol, ethanol and acetone, and insoluble in water. IR (KBr): 3482 ν (NH), 1677 ν (C=O), 1638 ν (C=O), 1601 ν (C=O...H), 1579 ν (C=N) cm⁻¹. ¹H-NMR (300.130 MHz) in DMSO, internal TMS, δ (ppm): 2.45 (s, 3H, CH₃), 2.46 (s, 3H, CH₃), 7.17–8.01 (m, 4H, Ar–H), 15.71 (s, 1H, N–H). ¹³C-¹H} NMR (75.468 MHz) in DMSO, internal TMS, δ (ppm): 26.47 (CH₃), 31.10 (CH₃), 114.83 (Ar–CC=O), 120.70 (Ar–NH–N), 123.72 (Ar–H), 131.45 (Ar–H), 132.64 (Ar–H), 134.28 (Ar–H), 143.40 (C=N), 168.17 (C=O), 194.94 (C=O), 196.74 (C=O).

HL⁷ (7). Yield 79% (based on pentane-2,4-dione), yellow powder soluble in DMSO, methanol, ethanol and acetone, and insoluble in water. IR (KBr): 3433 ν (NH), 1686 ν (C=O), 1644 ν (C=O...H), 1604 ν (C=N) cm⁻¹. ¹H-NMR (300.130 MHz) in DMSO, internal TMS, δ (ppm): 2.08 (s, 3H, CH₃), 2.37 (s, 3H, CH₃), 7.15–7.96 (4H, Ar–H), 12.38 (s, 1H, N–H). ¹³C-¹H} NMR (75.468 MHz) in DMSO, internal TMS, δ (ppm): 24.02 (CH₃), 30.77 (CH₃), 117.44 (Ar–H), 117.44 (Ar–H), 122.39 (Ar–NH–N), 125.02 (Ar–H), 125.02 (Ar–H), 134.75 (C=N), 138.28 (Ar–NO₂), 174.38 (C=O), 206.704 (C=O).

HL⁸ (8). Yield 86% (based on pentane-2,4-dione), yellow powder soluble in DMSO, methanol, ethanol and acetone, and insoluble in water. IR (KBr): 3434 ν (NH), 1678 ν (C=O), 1629 ν (C=O...H), 1603 ν (C=N) cm⁻¹. ¹H-NMR (300.130 MHz) in DMSO, internal TMS, δ (ppm): 2.08 (s, 3H, CH₃), 2.43 (s, 3H, CH₃), 7.16–7.56 (5H, Ar–H), 13.93 (s, 1H, N–H). ¹³C-¹H} NMR (75.468 MHz) in DMSO, internal TMS, δ (ppm): 28.82

(CH₃), 30.71 (CH₃), 116.37 (Ar–H), 125.36 (Ar–H), 125.36 (Ar–H), 129.29 (Ar–H), 129.57 (Ar–H), 133.36 (C=N), 142.10 (Ar–NH–N), 191.06 (C=O), 196.36 (C=O).

Syntheses of copper(II) complexes

Syntheses of 9, 13. 1 mmol of **2**, **6** was dissolved in water or in an acetone–water mixture (4 : 1, v/v) in the case of **6**, then 1 mmol of Cu(NO₃)₂·2.5H₂O was added. The mixture was stirred under solvent reflux for 5 min and left for slow evaporation; the greenish–black crystals of the product started to form after *ca.* 4 d at room temperature; they were then filtered off and dried in air.

[Cu₂(H₂O)₂(μ-HL²)₂] (9). Yield, 54% (based on Cu). Calcd. for C₁₁H₁₃AsCuN₂O₆ (*M* = 407.7): C 32.41, H 3.21, N 6.87; found C 32.32, H 3.18, N 6.80. MS (ESI): *m/z*: 389.8 [M+H]⁺. IR (KBr): 3368 (s, br) ν(OH), 1660 (s) ν(C=O), 1557 (s) ν(C=N) cm⁻¹.

[Cu(μ-L⁶)_n] (13). Yield, 69% (based on Cu). Calcd. for C₁₂H₁₀CuN₂O₄ (*M* = 309.76): C 46.53, H 3.25, N 9.04; found C 46.87, H 3.16, N 9.03. MS (ESI): *m/z*: 309.9 [M+H]⁺. IR (KBr): 3433 (s, br) ν(OH), 1673 (s) ν(C=O), 1637 (s) ν(C=O), 1598 (s) ν(C=N) cm⁻¹.

Synthesis of 10. Method A (Scheme 6, Route I): 1 mmol of **4** was dissolved in water (pH 6) then 1 mmol of Cu(NO₃)₂·2.5H₂O was added and the reaction mixture heated to 393 K for 5 min and then left at room temperature for slow evaporation; crystals of **10** suitable for X-rays started to form after *ca.* 4 d. Method B (Scheme 6, Route VII): 1 mmol of **12** was dissolved in water (pH 6) and then 1 mmol of Cu(NO₃)₂·2.5H₂O was added. The mixture was heated to 393 K for 5 min and then left at room temperature for slow evaporation; deep green crystals of **10** suitable for X-rays started to form after *ca.* 5 d.

[CuL⁴(H₂O)₂]H₂O (10). Yield, 65% (based on Cu). Calcd. for C₁₁H₁₆CuN₂O₈S (*M* = 399.9): C 33.04, H 4.03, N 7.01; found C 32.62, H 3.90, N 6.93. MS (ESI): *m/z*: 360.8 [M+H]⁺. IR (KBr): 3517 (s, br) ν(OH), 1644 (s) ν(C=O), 1586 (s) ν(C=O), 1547 (s) ν(C=N) cm⁻¹.

Synthesis of 11. Method A (Scheme 6, Route II): 1 mmol of **4** was dissolved in water and then 1 mmol of Cu(NO₃)₂·2.5H₂O and 0.1 M water solution of NH₄OH to reach pH 9 was added. The reaction mixture was stirred under solvent reflux for 5 min and left at room temperature for slow evaporation; crystals of **11** suitable for X-rays started to form after *ca.* 4 d. Method B (Scheme 6, Route II): 1 mmol of **12** was dissolved in water then 1 mmol of Cu(NO₃)₂·2.5H₂O and 0.1 M water solution of NH₄OH to reach pH 9 were added. The system was then left at room temperature for slow evaporation; crystals of **12** suitable for X-rays started to form after *ca.* 4 d.

[CuL⁴(H₂O)₂] (11). Yield, 60% (based on Cu). Calcd. for C₁₁H₁₄CuN₂O₇S (*M* = 381.8): C 34.60, H 3.70, N 7.34; found C 34.43, H 4.17, N 7.50. IR (KBr): 3436 (s, br) ν(OH), 1677 (s) ν(C=O), 1646 (s) ν(C=O), 1578 (s) ν(C=N) cm⁻¹.

Synthesis of 12. Method A (Scheme 5, Route III): 2 mmol of **4** were dissolved in water and then 1 mmol of Cu(NO₃)₂·2.5H₂O and 1 M water solution of HCl to reach pH 2 was added. The reaction mixture was stirred under solvent reflux for 5 min and left at room temperature for slow evaporation; crystals of **12** suitable for X-rays started to form after *ca.* 4 d. Method B (Scheme 6, Routes IV and

VI): 1 mmol of **10** or **11** was dissolved in water and then 1 mmol of **4** and 1 M water solution of HCl to reach pH 2 was added. The system was left at room temperature for slow evaporation; crystals of **12** suitable for X-rays started to form after *ca.* 4 d.

[Cu(HL⁴)₂(H₂O)₄] (12). Yield, 57% (based on Cu). Calcd. for C₁₁H₁₁CuN₂O₅S (*M* = 702.2): C 37.63, H 4.31, N 7.98; found C 37.52, H 4.20, N 7.80. MS (ESI): *m/z*: 682.7 [M+H]⁺. IR (KBr): 3437 (s, br) ν(OH), 1676 (s) ν(C=O), 1638 (s) ν(C=O), 1577 (s) ν(C=N) cm⁻¹.

Synthesis of 14 (Scheme 6, Route VIII). 2 mmol of **4** were dissolved in water, and then 1 mmol of Cu(NO₃)₂·2.5H₂O and 2 mmol of cyanoguanidine were added and stirred under solvent reflux for 5 min. After *ca.* 4 d at room temperature, light-green crystals precipitated which were then filtered off and dried in air.

[Cu(H₂O)₄{NCNC(NH₂)₂}]₂(HL⁴)₂(H₂O)₆ (14). Yield, 61% (based on Cu). Calcd. for C₂₆H₃₈CuN₁₂O₁₄S₂ (*M* = 870.3): C 35.88, H 4.40, N 19.31; found C 36.50, H 4.22, N 19.63. IR (KBr): 3450 (s, br) ν(OH), 2253 (s) ν(C≡N), 2209 (s) ν(C≡N), 1673 (s) ν(C=O), 1651 (s) ν(C=O), 1552 (s) ν(C=N) cm⁻¹.

Synthesis of 15 (Scheme 6, Route VIII or IX). 1 mmol of **4** was dissolved in water, and then 1 mmol of Cu(NO₃)₂·2.5H₂O and 1 mmol of cyanoguanidine or imidazole were added and stirred under solvent reflux for 5 min. After *ca.* 4 d the formed grey crystals were filtered off and dried in air.

[Cu(μ-L⁴)(NCHCHNHCH)]_n (15). Yield, 53% (based on Cu). Calcd. for C₁₄H₁₄CuN₄O₅S (*M* = 413.9): C 40.63, H 3.41, N 13.54; found C 40.88, H 3.38, N 13.38. IR (KBr): 3135 (s, br) ν(NH), 1668 (s) ν(C=O), 1653 (s) ν(C=O), 1588 (s) ν(C=N) cm⁻¹.

X-ray measurements

The crystals of **9–15** were immersed in cryo-oil, mounted in a Nylon loop, and measured at a temperature of 100 K. The X-ray diffraction data were collected on a Bruker Kappa Apex II (**9**), Bruker Smart Apex II²² (**10**, **11**, **14**), or Bruker Kappa Apex II Duo (**12**, **13**, **15**) CCD diffractometer using Mo–Kα radiation (λ = 0.710 73 Å). The *EvalCCD* (**9**) or *SAINT* (**10–15**) programs were used for cell refinements and data reductions. The structures were solved by direct methods using the *SHELXS-97* (**10**, **11**, **12**, **14**, **15**), *SIR97* (**9**) or *SIR2008* (**13**) programs with the *WinGX* graphical user interface.^{23–25} A semi-empirical absorption correction (*SADABS*)²⁶ was applied to all data. Structural refinements were carried out using *SHELXL-97*.²⁴ In **15** the imidazole ring was disordered over two sites with occupancies 0.51 and 0.49. The nitrogen atoms N3 and N3B as well as N4 and N4B were constrained to have equal coordinates and anisotropic displacement parameters. The OH, H₂O, NH₂, and NH (except in **15**) hydrogen atoms were located from the difference Fourier map but constrained to ride on their parent atom with U_{iso} = 1.5 U_{eq} (parent atom). Other hydrogen atoms were positioned geometrically and constrained to ride on their parent atoms, with C–H = 0.95–0.99 Å, N–H = 0.88 Å (the imidazole NH in **15**) and U_{iso} = 1.2–1.5 U_{eq} (parent atom). The crystallographic details are summarized in Table 6. CCDC 798948–798954 contain the supplementary crystallographic data for this paper.† These data can be obtained free of charge from The Cambridge Crystallographic Data Centre via www.ccdc.cam.ac.uk/data_request/cif.

Table 6 Crystal data and structure refinement details for compounds **9–15**

	9	10	11	12	13	14	15
Empirical formula	C ₂₂ H ₃₆ As ₂ Cu ₂ N ₄ O ₁₂	C ₂₂ H ₃₂ Cu ₂ N ₄ O ₁₆ S ₂	C ₁₁ H ₁₄ CuN ₂ O ₇ S	C ₂₂ H ₃₀ CuN ₄ O ₁₄ S ₂	C ₁₂ H ₁₀ CuN ₂ O ₄	C ₂₆ H ₅₀ CuN ₁₂ O ₂₀ S ₂	C ₁₄ H ₁₄ CuN ₄ O ₅ S
<i>F</i> w	815.39	799.72	381.84	702.16	309.76	978.44	413.89
Temp (K)	100(2)	100(2)	100(2)	100(2)	100(2)	100(2)	100(2)
λ (Å)	0.71073	0.71073	0.71073	0.71073	0.71073	0.71073	0.71073
Cryst syst	Triclinic	Monoclinic	Orthorhombic	Monoclinic	Monoclinic	Triclinic	Triclinic
Space group	$P\bar{1}$	$P2_1/n$	$Pbca$	$P2_1/n$	$P2_1/c$	$P\bar{1}$	$P\bar{1}$
<i>a</i> (Å)	7.9753(4)	11.3561(3)	15.222(7)	9.6052(2)	11.5658(13)	6.9100(6)	4.9947(3)
<i>b</i> (Å)	9.0989(4)	9.1757(3)	7.432(2)	13.5156(2)	5.2797(6)	12.0491(13)	8.5337(5)
<i>c</i> (Å)	10.3280(6)	15.5166(4)	26.225(9)	11.6369(2)	18.662(2)	14.337(2)	19.0626(10)
α (deg)	112.022(4)	90	90	90	90	108.578(7)	87.866(3)
β (deg)	94.776(6)	110.876(2)	90	108.9336(8)	90.281(4)	100.618(7)	82.974(3)
γ (deg)	98.031(4)	90	90	90	90	104.892(5)	76.536(3)
<i>V</i> (Å ³)	680.42(6)	1510.69(7)	2966.9(19)	1428.97(4)	1139.6(2)	1046.3(2)	784.21(8)
<i>Z</i>	1	2	8	2	4	1	2
ρ_{calc} (Mg m ⁻³)	1.990	1.758	1.710	1.632	1.805	1.553	1.753
μ (Mo K α) (mm ⁻¹)	4.047	1.628	1.649	0.987	1.928	0.713	1.561
No. reflns.	11 269	23 254	11 212	20 758	6932	8178	14341
Unique reflns.	3962	7238	2603	3795	2149	4674	4783
GOOF (<i>F</i> ²)	1.085	1.024	1.037	1.056	0.970	0.854	1.030
<i>R</i> _{int}	0.0340	0.0340	0.0916	0.0304	0.0624	0.0473	0.0397
<i>R</i> ^a (<i>I</i> ≥ 2 σ)	0.0323	0.0309	0.0535	0.0301	0.0441	0.0432	0.0416
<i>wR</i> ^b (<i>I</i> ≥ 2 σ)	0.0680	0.0765	0.1294	0.0774	0.1218	0.0705	0.0912

^a $R1 = \sum \|F_o\| - |F_c| / \sum \|F_o\|$. ^b $wR2 = [\sum [w(F_o^2 - F_c^2)^2] / \sum [w(F_o^2)^2]]^{1/2}$.

Computational details

The full geometry optimization of all structures has been carried out at the DFT/HF hybrid level of theory using the B3LYP functional²⁷ and 6-31+G(d) basis set with the help of the Gaussian-98²⁸ program package. Restricted approximations for the structures with closed electron shells and unrestricted methods for the structures with open electron shells have been employed. No symmetry operations have been applied. The Hessian matrix was calculated analytically for the optimized structures in order to prove the location of correct minima (no imaginary frequencies), and to estimate the thermodynamic parameters, the latter being calculated at 298.15 K. Vertical ionization potentials (IP) and vertical electron affinities (EA) were calculated using the formulae (1) and (2):

$$\text{IP} = E(\text{A}^+) - E(\text{A}) \quad (1)$$

$$\text{EA} = E(\text{A}) - E(\text{A}^-) \quad (2)$$

where *E*(A) is the total energy of the neutral structure **1–8**, and *E*(A⁺) and *E*(A⁻) are the total energies of the oxidized and reduced species with the geometry corresponding to that of the neutral structure **1–8**.

Total energies corrected for solvent effects (*E*_s) were estimated at the single-point calculations on the basis of gas-phase geometries using the polarizable continuum model²⁹ in the CPCM version³⁰ with water as solvent. The entropic term in solutions (*S*_s) was calculated according to the procedure described by Wertz³¹ and Cooper and Ziegler³² using equation $S_s = S_g + [(-14.3 \text{ cal mol}^{-1} \text{ K}^{-1}) - 0.46(S_g - 14.3 \text{ cal mol}^{-1} \text{ K}^{-1}) + 7.98 \text{ cal mol}^{-1} \text{ K}^{-1}]$ where *S*_g is gas-phase entropy of solute. The enthalpies and Gibbs free energies in solution (*H*_s and *G*_s) were estimated using the equations $H_s = E_s + H_g - E_g$ and $G_s = H_s - TS_s$ where *E*_g and *H*_g are gas-phase total energy and enthalpy.

To estimate the relative stabilities of some complexes, the ΔG_s values of the model reactions of complex formation from [Cu(OH)₂(H₂O)₂] and the ligand (Scheme 7) have been calculated. The penta-coordinated tetragonal pyramid structures were selected as the starting geometries of the complexes, in accordance with the experimental X-ray data.^{8c} In the case of [Cu(L¹)(H₂O)₂]-H₂O and [Cu(L⁴)(H₂O)₂]-H₂O, the coordination polyhedron was preserved during the optimization. The optimization of [Cu(OH)(L⁸)(H₂O)₂] resulted in the extrusion of an axial water molecule from the inner coordination sphere and formation of the complex [Cu(OH)(L⁸)(H₂O)]-H₂O. Two factors determined the selection of the model reactions (Scheme 7). First, the charged species were avoided to minimize computational errors of the solvent effect. Second, the number of species before and after reaction was selected to be the same to minimize errors in the entropy term.

Oxidation of cyclohexane

The reaction mixtures were prepared as follows: to 4.9–10.0 μmol of the complex **9**, **10**, **12** or **13** contained in the reaction flask were added 4 mL of MeCN, 0–0.60 mmol of HNO₃, 1.00 mmol of C₆H₁₂ and 5.00–12.5 mmol of H₂O₂ solution (30% in H₂O), in this order. The reaction mixture was stirred for 6 h at room temperature (*ca.* 298 K) and air atmospheric pressure, then 90 μL of cycloheptanone (as internal standard) and 5.0 mL of diethyl ether (to extract the substrate and the products from the reaction mixture) were added. The resulting mixture was stirred for 15 min and then a sample taken from the organic phase was analyzed by GC. Subsequently, PPh₃ was added to the final organic phase (to reduce the cyclohexyl hydroperoxide, if formed), the mixture was analyzed again to estimate the amount of cyclohexyl hydroperoxide, according to Shul'pin's method.¹⁸ Blank experiments were performed and confirmed that no cyclohexane

oxidation products were obtained in the absence of the metal catalyst.

Acknowledgements

This work has been partially supported by the Foundation for Science and Technology (FCT), Portugal, and its PPCDT (FEDER funded) and "Science 2007" programs. The authors acknowledge the Portuguese NMR Network for providing access to the NMR facility.

References

- (a) F. R. Japp and F. Klingemann, *Liebigs Ann. Chem.*, 1888, **247**, 190; (b) H. C. Yao and P. Resnick, *J. Am. Chem. Soc.*, 1962, **84**, 3514; (c) H. C. Yao, *J. Org. Chem.*, 1964, **29**, 2959.
- (a) H. B. Hassib, Y. M. Issa and W. S. Mohamed, *J. Therm. Anal. Calorim.*, 2008, **92**, 775; (b) H. G. Garg and R. A. Sharma, *J. Med. Chem.*, 1970, **13**, 763; (c) H. G. Garg and R. A. Sharma, *J. Med. Chem.*, 1970, **13**, 763; (d) Z. Chen, Y. Wu, D. Gu and F. Gan, *Dyes Pigm.*, 2008, **76**, 624; (e) E. V. Shchegol'kov, O. G. Khudina, L. V. Anikina, Ya. V. Burgart and V. I. Saloutin, *Pharm. Chem. J.*, 2006, **40**, 373; (f) E. E. Oruch, B. Kochyigit-Kaymakchoglu, B. Oral, H. Z. Altunbas-Toklu, L. Kabasakal and S. Rollas, *Arch. Pharm.*, 2006, **339**, 267; (g) S. C. Nigam, G. S. Saharia and H. R. Sharma, *Def. Sci. J.*, 1982, **32**, 87; (h) G. Sh. Kuchukguzel, S. Rollas, I. Kuchukguzel and M. Kiraz, *Eur. J. Med. Chem.*, 1999, **34**, 1093; (i) E. S. H. El Ashry, L. F. Awad, E. I. Ibrahim and O. Kh. Bdeewy, *Chin. J. Chem.*, 2007, **25**, 570; (j) J. Sokolnicki, J. Legendziewicz, W. Amirkhanov, V. Ovchinnikov, L. Macalik and J. Hanuza, *Spectrochim. Acta, Part A*, 1999, **55**, 349.
- (a) F. Huang, Y. Wu, D. Gu and F. Gan, *Thin Solid Films*, 2005, **483**, 251; (b) Z. Chen, F. Huang, Y. Wu, D. Gu and F. Gan, *Inorg. Chem. Commun.*, 2006, **9**, 21.
- (a) O. A. Attanasi, P. Filippone, C. Fiorucci and F. Mantellini, *Tetrahedron Lett.*, 1999, **40**, 3891; (b) E. V. Shchegol'kov, Y. V. Burgart, O. G. Khudina, V. I. Saloutin and O. N. Chupakhin, *Russ. Chem. Bull.*, 2004, **53**, 2584; (c) A.-Z. A. Elassar, H. H. Dib, N. A. Al-Awadi and M. H. Elnagdi, *Arkivoc*, 2007, (ii), 272; (d) O. G. Khudina, E. V. Shchegol'kov, Ya. V. Burgart, V. I. Saloutin, D. V. Bukhvalov, D. V. Starichenko, Yu. N. Shvachko, A. V. Korolev, V. V. Ustinov, G. G. Aleksandrov, I. L. Eremenko, O. N. Kazheva, G. V. Shilov, O. A. Dyachenko and O. N. Chupakhin, *Rus. Chem. Bull., Int. Ed.*, 2007, **56**, 108; (e) D. Z. Mijin, M. Baghbanzadeh, C. Reidlinger and C. O. Kappe, *Dyes Pigm.*, 2010, **85**, 73.
- (a) R. A. Aliyeva, F. M. Chyragov and K. T. Mahmudov, *J. Anal. Chem.*, 2005, **50**, 137; (b) S. R. Gadjeva, T. M. Mursalov, K. T. Mahmudov, F. G. Pashaev and F. M. Chyragov, *J. Anal. Chem.*, 2006, **61**, 550; (c) S. R. Gadjeva, K. T. Mahmudov and F. M. Chyragov, *J. Anal. Chem.*, 2006, **61**, 634; (d) S. R. Gadjeva, F. M. Chyragov and K. T. Mahmudov, *J. Anal. Chem.*, 2007, **62**, 1028; (e) K. T. Mahmudov, R. A. Aliyeva, S. R. Gadjeva and F. M. Chyragov, *J. Anal. Chem.*, 2008, **63**, 435.
- (a) P. Gilli, L. Pretto, V. Bertolasi and G. Gilli, *Acc. Chem. Res.*, 2009, **42**, 33; (b) P. Simunek, V. Bertolasi and V. Machacek, *J. Mol. Struct.*, 2002, **642**, 41; (c) P. Gilli, V. Bertolasi, L. Pretto, A. Lycka and G. Gilli, *J. Am. Chem. Soc.*, 2002, **124**, 13554; (d) P. Gilli, V. Bertolasi, L. Pretto and G. Gilli, *J. Mol. Struct.*, 2006, **790**, 40.
- P. Sanz, O. Mo, M. Yanez and J. Elguero, *Chem.-Eur. J.*, 2008, **14**, 4225.
- (a) A. M. Maharramov, R. A. Aliyeva, I. A. Aliyev, F. G. Pashaev, A. G. Gasanov, S. I. Azimova, R. K. Askerov, A. V. Kurbanov and K. T. Mahmudov, *Dyes Pigm.*, 2010, **85**, 1; (b) J. Marten, W. Seichter and E. Weber, *Z. Anorg. Allg. Chem.*, 2005, **631**, 869; (c) E. Weber, J. Marten and W. Seichter, *J. Coord. Chem.*, 2009, **62**, 3401; (d) K. T. Mahmudov, M. N. Kopylovich, M. F. C. Guedes da Silva, P. J. Figiel, Y. Y. Karabach and A. J. L. Pombeiro, *J. Mol. Catal. A: Chem.*, 2010, **318**, 44; (e) M. N. Kopylovich, K. T. Mahmudov, M. F. C. Guedes da Silva, M. L. Kuznetsov, P. J. Figiel, Y. Y. Karabach, K. V. Luzyanin and A. J. L. Pombeiro, *Inorg. Chem.*, 2011, **50**, 918.
- (a) A. E. Shilov and G. B. Shul'pin, *Chem. Rev.*, 1997, **97**, 2879; (b) G. B. Shul'pin, *Oxidations of C-H Compounds Catalyzed by Metal Complexes, in Transition Metals for Organic Synthesis*, M. Beller, C. Bolm, ed., Wiley-VCH: Weinheim/New York, 2nd edition, 2004, vol. 2, pp. 215–242; (c) G. B. Shul'pin, *Mini-Rev. Org. Chem.*, 2009, **6**, 95.
- (a) A. M. Kirillov, M. N. Kopylovich, M. V. Kirillova, M. Haukka, M. F. C. Guedes da Silva and A. J. L. Pombeiro, *Angew. Chem., Int. Ed.*, 2005, **44**, 4345; (b) A. M. Kirillov, Y. Y. Karabach, M. Haukka, M. F. C. Guedes da Silva, J. Sanchiz, M. N. Kopylovich and A. J. L. Pombeiro, *Inorg. Chem.*, 2008, **47**, 162; (c) S. Contaldi, C. Di Nicola, F. Garau, Y. Y. Karabach, L. M. D. R. S. Martins, M. Monari, L. Pandolfo, C. Pettinari and A. J. L. Pombeiro, *Dalton Trans.*, 2009, 4928; (d) G. V. Nizova, B. Krebs, G. Suss-Fink, S. Schindler, L. Westerheide, L. G. Cuervo and G. B. Shul'pin, *Tetrahedron*, 2002, **58**, 9231; (e) G. B. Shul'pin, Y. N. Kozlov, G. V. Nizova, G. Suss-Fink, S. Stanislas, A. Kitaygorodskiy and V. S. Kulikova, *J. Chem. Soc., Perkin Trans. 2*, 2001, **2**, 1351; (f) G. Suss-Fink, L. Gonzalez and G. B. Shul'pin, *Appl. Catal., A*, 2001, **217**, 111; (g) G. B. Shul'pin and G. Suss-Fink, *J. Chem. Soc., Perkin Trans. 2*, 1995, **2**, 1459; (h) M. Kodera, H. Shimakoshi and K. Kano, *Chem. Commun.*, 1996, 1737.
- (a) L. M. Mirica, X. Ottenwaelder and T. D. P. Stack, *Chem. Rev.*, 2004, **104**, 1013; (b) S. J. Elliot, M. Zhu, L. Tso, H.-H. T. Nguyen, J. H.-K. Yip and S. I. Chan, *J. Am. Chem. Soc.*, 1997, **119**, 9949; (c) R. L. Lieberman and A. C. Rosenzweig, *Nature*, 2005, **434**, 177.
- (a) V. Bertolasi, P. Gilli, V. Ferretti, G. Gilli and K. Vaughan, *New J. Chem.*, 1999, **23**, 1261; (b) J. Marten, W. Seichter, E. Weber and U. Bohme, *J. Phys. Org. Chem.*, 2007, **20**, 716.
- M. N. Kopylovich, K. T. Mahmudov, M. F. C. G. Silva, L. M. D. R. S. Martins, M. L. Kuznetsov, T. F. S. Silva, J. J. R. F. Silva and A. J. L. Pombeiro, *J. Phys. Org. Chem.*, 2011, **24**, DOI: 10.1002/poc.1824.
- (a) H. M. Cordes, *J. Phys. Chem.*, 1968, **72**, 2185; (b) J. Sestak, *Thermodynamical Properties of Solids* Academia: Prague, 1984; (c) J. M. Criado, L. A. Perez-Maqueda and P. E. Sanchez-Jimenez, *J. Therm. Anal. Calorim.*, 2005, **82**, 671.
- (a) L. Q. Hatcher, D. H. Lee, M. A. Vance, A. E. Milligan, R. Sarangi, K. O. Hodgson, B. Hedman, E. I. Solomon and K. D. Karlin, *Inorg. Chem.*, 2006, **45**, 10055; (b) T. Matsumoto, H. Furutachi, S. Nagatomo, T. Tosha, S. Fujinami, T. Kitagawa and M. Suzuki, *J. Organomet. Chem.*, 2007, **692**, 111; (c) D. Maiti, H. C. Fry, J. S. Woertink, M. A. Vance, E. I. Solomon and K. D. Karlin, *J. Am. Chem. Soc.*, 2007, **129**, 264; (d) H. R. Lucas, L. Li, A. A. N. Sarjeant, M. A. Vance, E. I. Solomon and K. D. Karlin, *J. Am. Chem. Soc.*, 2009, **131**, 3230.
- (a) E. A. Lewis and W. B. Tolman, *Chem. Rev.*, 2004, **104**, 1047; (b) R. W. Cruse, S. Kaderli, C. J. Meyer, A. D. Zuberbuehler and K. D. Karlin, *J. Am. Chem. Soc.*, 1988, **110**, 5020.
- (a) M. V. Kirillova, Y. N. Kozlov, L. S. Shul'pina, O. Y. Lyakin, A. M. Kirillov, E. P. Talsi, A. J. L. Pombeiro and G. B. Shul'pin, *J. Catal.*, 2009, **268**, 26; (b) A. M. Kirillov, M. N. Kopylovich, M. V. Kirillova, Y. Y. Karabach, M. Haukka, M. F. C. Guedes da Silva and A. J. L. Pombeiro, *Adv. Synth. Catal.*, 2006, **348**, 159; (c) D. S. Nesterov, V. N. Kozozay, V. V. Dyakonov, O. V. Shishkin, J. Jezierski, A. Ozarowski, A. M. Kirillov, M. N. Kopylovich and A. J. L. Pombeiro, *Chem. Commun.*, 2006, 4605; (d) L. M. Slaughter, J. P. Collman, T. A. Eberspacher and J. I. Brauman, *Inorg. Chem.*, 2004, **43**, 5198; (e) M. V. Kirillova, A. M. Kirillov, M. F. C. Guedes da Silva and A. J. L. Pombeiro, *Eur. J. Inorg. Chem.*, 2008, **22**, 3423; (f) A. M. Kirillov, M. Haukka, M. F. C. Guedes da Silva and A. J. L. Pombeiro, *Eur. J. Inorg. Chem.*, 2005, **11**, 2071; (g) G. B. Shul'pin, *J. Mol. Catal. A: Chem.*, 2005, **227**, 247; (h) Y. N. Kozlov, V. B. Romakh, A. Kitaygorodskiy, P. Buglyo, G. Suss-Fink and G. B. Shul'pin, *J. Phys. Chem. A*, 2007, **111**, 7736.
- (a) G. B. Shul'pin, *J. Mol. Catal. A: Chem.*, 2002, **189**, 39; (b) G. B. Shul'pin, M. G. Matthes, V. B. Romakh, M. I. F. Barbosa, J. L. T. Aoyagi and D. Mandelli, *Tetrahedron*, 2008, **64**, 2143; (c) Y. Y. Karabach, A. M. Kirillov, M. Haukka, M. N. Kopylovich and A. J. L. Pombeiro, *J. Inorg. Biochem.*, 2008, **102**, 1190; (d) C. Di Nicola, Y. Y. Karabach, A. M. Kirillov, M. Monari, L. Pandolfo, C. Pettinari and A. J. L. Pombeiro, *Inorg. Chem.*, 2007, **46**, 221; (e) M. V. Kirillova, A. M. Kirillov, P. M. Reis, J. A. L. Silva, J. J. R. Frausto da Silva and A. J. L. Pombeiro, *J. Catal.*, 2007, **248**, 130; (f) G. B. Shul'pin, *C. R. Chim.*, 2003, **6**, 163; (g) M. Costas, M. P. Mehn, M. P. Jensen and L. Que, Jr., *Chem. Rev.*, 2004, **104**, 939; (h) G. B. Shul'pin, H. Stoeckli-Evans, D. Mandelli, Y. N. Kozlov, A. T. Vallina, C. B. Woitiski, R. S. Jimenez and W. A. Carvalho, *J. Mol. Catal. A: Chem.*, 2004, **219**, 255; (i) G. B. Shul'pin, Y. N. Kozlov, G. V. Nizova, G. Suss-Fink, S. Stanislas, A. Kitaygorodskiy and V. S. Kulikova, *J. Chem. Soc., Perkin. Trans. 2*, 2001, 1351.
- (a) T. F. S. Silva, E. C. B. A. Alegria, L. M. D. R. S. Martins and A. J. L. Pombeiro, *Adv. Synth. Catal.*, 2008, **350**, 706; (b) T. F. S. Silva, G. S.

- Mishra, M. F. Guedes da Silva, R. Wanke, L. M. D. R. S. Martins and A. J. L. Pombeiro, *Dalton Trans.*, 2009, 9207.
- 20 (a) R. Raja and P. Ratnasamy, *Catal. Lett.*, 1997, **48**, 1; (b) S. Velusamy and T. Punniyamurthy, *Tetrahedron Lett.*, 2003, **44**, 8955.
- 21 A. J. L. Pombeiro, M. F. C. Guedes da Silva and M. A. N. D. A. Lemos, *Coord. Chem. Rev.*, 2001, **219–221**, 53.
- 22 Bruker AXS, *APEX2 - Software Suite for Crystallographic Programs*, Bruker AXS, Inc., Madison, WI, USA, 2009.
- 23 M. C. Burla, M. Camalli, B. Carrozzini, G. L. Casciarano, C. Giacovazzo, G. Polidori and R. Spagna, *J. Appl. Crystallogr.*, 2005, **38**, 381.
- 24 G. M. Sheldrick, *Acta Crystallogr., Sect. A: Found. Crystallogr.*, 2008, **64**, 112.
- 25 L. J. Farrugia, *J. Appl. Crystallogr.*, 1999, **32**, 837.
- 26 G. M. Sheldrick, *SADABS - Bruker Nonius scaling and absorption correction*, Bruker AXS, Inc., Madison, Wisconsin, USA, 2008.
- 27 (a) A. D. Becke, *J. Chem. Phys.*, 1993, **98**, 5648; (b) C. Lee, W. Yang and R. G. Parr, *Phys. Rev.*, 1988, **B37**, 785.
- 28 M. J. Frisch, G. W. Trucks, H. B. Schlegel, G. E. Scuseria, M. A. Robb, J. R. Cheeseman, V. G. Zakrzewski, J. A. Jr. Montgomery, R. E. Stratmann, J. C. Burant, S. Dapprich, J. M. Millam, A. D. Daniels, K. N. Kudin, M. C. Strain, O. Farkas, J. Tomasi, V. Barone, M. Cossi, R. Cammi, B. Mennucci, C. Pomelli, C. Adamo, S. Clifford, J. Ochterski, G. A. Peterson, P. Y. Ayala, Q. Cui, K. Morokuma, D. K. Malick, A. D. Rabuck, K. Raghavachari, J. B. Foresman, J. Cioslowski, J. V. Ortiz, A. G. Baboul, B. B. Stefanov, G. Liu, A. Liashenko, P. Piskorz, I. Komaromi, R. Gomperts, R. L. Martin, D. J. Fox, T. Keith, M. A. Al-Laham, C. Y. Peng, A. Nanayakkara, M. Challacombe, P. M. W. Gill, B. Johnson, W. Chen, M. W. Wong, J. L. Andres, C. Gonzalez, M. Head-Gordon, E. S. Replogle, J. A. Pople, *Gaussian 98*, revision A.9; Gaussian, Inc.: Pittsburgh PA, 1998.
- 29 J. Tomasi and M. Persico, *Chem. Rev.*, 1994, **94**, 2027.
- 30 V. Barone and M. Cossi, *J. Phys. Chem.*, 1998, **102**, 1995.
- 31 G. H. Wertz, *J. Am. Chem. Soc.*, 1980, **102**, 5316.
- 32 J. Cooper and T. Ziegler, *Inorg. Chem.*, 2002, **41**, 6614.